Screening of fatty alcohol dehydrogenase and its application on alkane production

SUI YU-AN

2023

CONTENTS

ABBREVIATIONS

Acyl-ACP	Acyl-acyl carrier protein
ADH	Alcohol dehydrogenase
ADO	Aldehyde-deformylating oxygenase (also called aldehyde decarbonylase)
ALR	Aldehyde reductase
AR	Acyl-ACP reductase
BLAST	Basic Local Alignment Search Tool
CFE	Cell-free extracts
CV	Column volume
DDBJ	DNA Data Bank of Japan
FAD	Flavin adenine dinucleotide
Fd	Ferredoxin
FNR	Ferredoxin $NADP^+$-reductase
FPLC	Fast protein liquid chromatography
GC	Gas chromatography
GC-MS	Gas chromatography-mass spectrometry
HMW	High molecular weight
IPTG	Isopropyl β-D-1-thiogalactopyranoside
kb	Kilobase
KPB	Potassium phosphate buffer
LB medium	Luria–Bertani medium
LC-MS	High performance liquid chromatography-mass spectrometry
LMW	Low molecular weight
MDR family	Medium-chain dehydrogenases/reductases family
M_r	Relative molecular mass

NAD^+	Nicotinamide adenine dinucleotide, oxidized
NADH	Nicotinamide adenine dinucleotide, reduced
$NADP^+$	Nicotinamide adenine dinucleotide phosphate, oxidized
NADPH	Nicotinamide adenine dinucleotide phosphate, reduced
NCBI	National Center for Biotechnology Information
OD_{600}	Optical density at 600 nm
PVDF membrane	Polyvinylidene difluoride membrane
SD	Standard deviation
SDS-PAGE	Sodium dodecyl sulfate–polyacrylamide gel electrophoresis
Tris	Tris(hydroxymethyl)aminomethane

GENERAL INTRODUCTION

Biofuels produced from renewable biomass are promising alternatives to fossil fuels (1, 2). Recently, bio-based hydrocarbons, such as alkanes and alkenes, have attracted particularly considerable attention since they share similar chemical composition with petroleum-based fuels and show better performance than other biofuels due to their higher energy content (3). Alkanes are produced by many organisms in nature, including plants, insects, and microorganisms, where in most cases, fatty aldehydes derived from fatty acid metabolism are converted to alkanes through a decarbonylation reaction mechanism (4–9). To date, there have been numerous reports on the production of medium-chain (C13–C17) alkanes from glucose using *Escherichia coli*, *Saccharomyces cerevisiae*, and other metabolic engineered microorganisms (10–14). For example, by introducing cyanobacterial acyl-ACP reductase (AR) and aldehyde-deformylating oxygenase (ADO) (also called aldehyde decarbonylase), alkane titer in *E. coli* reached 300 mg$\cdot$ l^{-1} (15).

A bottleneck in alkane production using *E. coli* as the host is caused by the endogenous aldehyde reductase, which converts intracellular aldehyde to alcohol (16, 17). The substrate pool for ADO was competed by aldehyde reductase, resulting in poor alkane production. It has been reported that the alkane titer increased nearly twofold by removing *yqhD*, a gene encoding aldehyde reductase found in *E. coli* (18). Also, it has been reported that up to 13 genes encoding aldehyde reductase are found in *E. coli*, and the deletion of these genes results in a 90% reduction in endogenous alcohol accumulation (19). However, it takes tremendous effort to conduct gene deletion, and the resulting aldehyde accumulation is toxic to the cell (19, 20). To avoid these concerns and to efficiently drive metabolic flow to alkane production, a better approach to utilize alcohol byproducts in *E. coli* remains necessary.

This study aims to construct a pathway linking alcohol oxidation with alkane biosynthesis. Coupling an alcohol dehydrogenase (ADH) capable of converting fatty alcohols to the corresponding fatty aldehydes with cyanobacterial AR and ADO (15, 21) could improve the alkane production by utilizing the alcohol as the substrate again. This study demonstrates such approach in three different stages, as shown in Scheme 1.

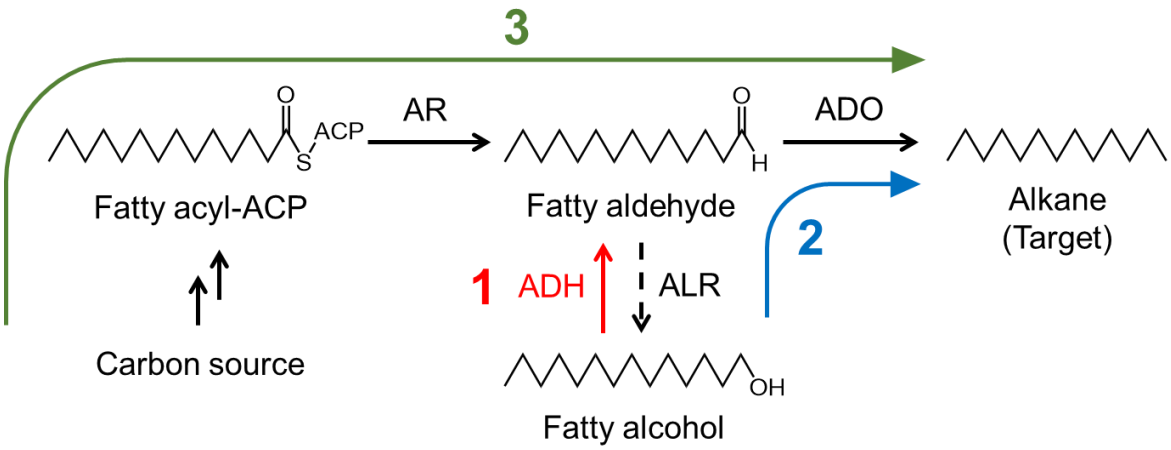

Scheme 1 Reactions involved in alkane biosynthetic pathway. The numbers indicate the chapters where the reactions were discussed. ADO, aldehyde-deformylating oxygenase. ALR, aldehyde reductase. AR, acyl-ACP reductase.

Chapter 1 focuses on the screening of 1-tetradecanol-oxidizing bacteria and the characterization of a fatty alcohol dehydrogenase. Chapter 2 focuses on the combined reaction of the newly found ADH with a cyanobacterial ADO to achieve the direct production of alkane from fatty alcohols. Chapter 3 focuses on the effect of introducing ADH to fermentative production of alkane.

Regarding the lack of research about utilizing fatty alcohol for alkane biosynthesis (22), this study will provide a new point of view for the development of biofuel. Besides, the enzyme found in this study can be applied to the biosynthetic pathway involving the formation of medium-chain aldehydes to produce alkanes and other valuable compounds.

REFERENCES

1. A. J. Ragauskas, C. K. Williams, B. H. Davison, G. Britovsek, J. Cairney, C. A. Eckert, W. J. J. Frederick, J. P. Hallett, D. J. Leak, C. L. Liotta, J. R. Mielenz, R. Murphy, R. Templer, T. Tschaplinsk. The path forward for biofuels and biomaterials. *Science* **311**:484–489 (2006).
2. P. P. Peralta-Yahya, F. Zhang, S. B. del Cardayre, J. D. Keasling. Microbial engineering for the production of advanced biofuels. *Nature* **488**:320–328 (2012).
3. R. M. Lennen, D. J. Braden, R. M. West, J. A. Dumesic, B. F. Pfleger. A process for microbial hydrocarbon synthesis: overproduction of fatty acids in *Escherichia coli* and catalytic conversion to alkanes. *Biotechnol. Bioeng.* **106**:193–202 (2010).
4. T. M. Cheesbrough, P. E. Kolattukudy. Alkane biosynthesis by decarbonylation of aldehydes catalyzed by a particulate preparation from *Pisum sativum*. *Proc. Natl. Acad. Sci. U.S.A.* **81**:6613–6617 (1984).
5. M. Dennis, P. E. Kolattukudy. A cobalt-porphyrin enzyme converts a fatty aldehyde to a hydrocarbon and CO. *Proc. Natl. Acad. Sci. U.S.A.* **89**:5306–5310 (1992).
6. J. A. Tillman, S. J. Seybold, R. A. Jurenka, G. J. Blomquist. Insect pheromones—an overview of biosynthesis and endocrine regulation. *Insect. Biochem. Mol. Biol.* **29**:481–514 (1999).
7. L. Samuels, L. Kunst, R. Jetter. Sealing plant surfaces: cuticular wax formation by epidermal cells. *Annu. Rev. Plant. Biol.* **59**:683–707 (2008).
8. B. Bourdenx, A. Bernard, F. Domergue, S. Pascal, A. Leger, D. Roby, M. Pervent, D. Vile, R. P. Haslem, J. A. Napier, R. Lessire, J. Joubes. Overexpression of Arabidopsis *ECERIFERUM1* promotes wax very-long-chain alkane biosynthesis and influences plant response to biotic and abiotic stresses. *Plant. Physiol.* **156**:29–45 (2011).
9. M. Ito, H. Kambe, S. Kishino, M. Muramatsu, J. Ogawa. A search for microorganisms producing medium-chain alkanes from aldehydes. *J. Biosci. Bioeng.* **125**:87–91 (2017).
10. Y. J. Choi, S. Y. Lee. Microbial production of short-chain alkanes. *Nature* **502**:571–574 (2013).
11. Y. X. Cao, W. H. Xiao, J. L. Zhang, Z. X. Xie, M. Z. Ding, Y. J. Yuan. Heterologous biosynthesis and manipulation of alkanes in *Escherichia coli*. *Metab. Eng.* **38**:19–28 (2016).
12. N. A. Buijs, Y. J. Zhou, V. Siewers, J. Nielsen. Long-chain alkane production by the yeast *Saccharomyces cerevisiae*. *Biotechnol. Bioeng.* **112**:1275–1279 (2015).
13. Y. J. Zhou, N. A. Buijs, Z. Zhu, J. Qin, V. Siewers, J. Nielsen. Production of fatty acid-derived oleochemicals and biofuels by synthetic yeast cell factories. *Nat. Commun.* **7**:11709 (2016).
14. H. M. Kim, T. U. Chae, S. Y. Choi, W. J. Kim, S. Y. Lee. Engineering of an oleaginous bacterium for the production of fatty acids and fuels. *Nat. Chem. Biol.* **15**:721–729 (2019).

15. A. Schirmer, M. A. Rude, X. Li, E. Popova, S. B. del Cardayre. Microbial biosynthesis of alkanes. *Science* **329**:559–562 (2010).
16. J. M. Perez, F. A. Arenas, G. A. Pradenas, J. M. Sandoval, C. C. Vasquez. *Escherichia coli* YqhD exhibits aldehyde reductase activity and protects from the harmful effect of lipid peroxidation-derived aldehydes. *J. Biol. Chem.* **283**:7346–7353 (2008).
17. Z. Fatma, K. Jawed, A. J. Mattam, S. S. Yazdani. Identification of long chain specific aldehyde reductase and its use in enhanced fatty alcohol production in *E. coli*. *Metab. Eng.* **37**:35–45 (2016).
18. X. Song, H. Yu, K. Zhu. Improving alkane synthesis in *Escherichia coli* via metabolic engineering. *Appl. Microbiol. Biotechnol.* **100**:757–767 (2016).
19. G. M. Rodriguez, S. Atsumi. Toward aldehyde and alkane production by removing aldehyde reductase activity in *Escherichia coli*. *Metab. Eng.* **25**:227–237 (2014).
20. A. W. Grant, G. Steel, H. Waugh, E. M. Ellis. A novel aldo-keto reductase from *Escherichia coli* can increase resistance to methylglyoxal toxicity. *FEMS Microbiol. Lett.* **218**:93–99 (2003).
21. B. Paul, D. Das, B. Ellington, E. N. G. Marsh. Probing the mechanism of cyanobacterial aldehyde decarbonylase using a cyclopropyl aldehyde. *J. Am. Chem. Soc.* **135**:5234–5237 (2013).
22. I. J. Cho, K. R. Choi, S. Y. Lee. Microbial production of fatty acids and derivative chemicals. *Curr. Opin. Biotechnol.* **65**:129–141 (2020).

CHAPTER 1

Screening of alcohol-oxidizing bacteria and characterization of alcohol dehydrogenase PsADH from *Pantoea* sp. 7-4

INTRODUCTION

The alkane production in metabolic engineered microorganisms, such as *E. coli*, was strongly limited by the endogenous aldehyde reductases which convert fatty aldehydes to fatty alcohols (1, 2). In this chapter, a screening of fatty alcohol-oxidizing bacteria was conducted in order to find an enzyme suitable for re-oxidizing the accumulated cellular fatty alcohols. The reaction scheme is shown in Scheme 1.1. 1-Tetradecanol, the carbon 14 saturated fatty alcohol, was selected as the substrate for the screening since its corresponding aldehyde product can be utilized as precursor for the downstream alkane biosynthesis generating the valuable tridecane product.

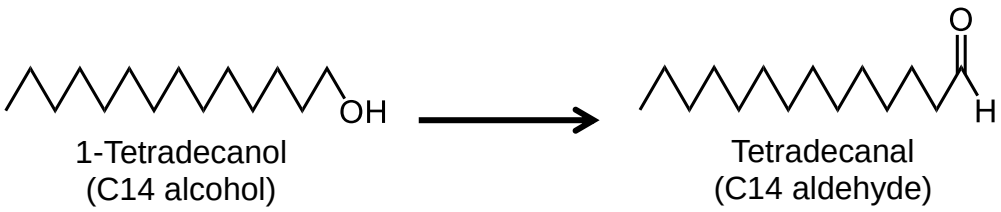

Scheme 1.1 Target reaction discussed in this chapter.

This chapter describes the discovery of an enzyme involved in the above reaction. The screening started with isolation of soil microorganisms followed by the identification of 1-tetradecanol-assimilating strains. By applying a series of column chromatography and enzyme assay, the target enzyme in the selected microorganism was purified, and the molecular biological information as well as the biochemical properties of this newly found enzyme was further revealed.

MATERIALS AND METHODS

Chemicals, microbial strains, nucleotide sequences, primers, and plasmids

1-Tetradecanol and tetradecanal were purchased from Tokyo Chemical Industry Co., LTD. (Tokyo, Japan). The NAD^+ disodium salt and $NADP^+$ tetrasodium salt were purchased from Oriental Yeast Co., LTD. (Tokyo, Japan). Yeast extract was purchased from BD Biosciences (Franklin Lakes, NJ, USA). Other reagents were purchased from Fujifilm Wako Pure Chemical Corporation (Osaka, Japan). The *E. coli* DH5α and *E. coli* Rosetta 2 (DE3) (Merck, Darmstadt, Germany) were used as the hosts for gene cloning and expression, respectively. The nucleotide sequences (Table S1.1) and the primers (Table S1.2) used in this chapter are shown in the supplementary information. The plasmid pET-21b (+), pRSFDuet-1, and pCDFDuet-1 (Merck) were used as the expression vectors. Other chemicals used in this study were of analytical grade and commercially available.

Isolation of 1-tetradecanol-assimilating microorganisms

Soil samples were collected from places all over Japan and used as the source for screening of isolation of 1-tetradecanol-assimilating microorganisms. First, soil samples were suspended in saline water and incubated at room temperature for 1 h. Approximately 20–30 µL of the supernatant of the solution was then inoculated into a 3 mL enrichment medium that consisted of 0.5% (w/v) $(NH_4)_2SO_4$, 0.1% (w/v) NH_4Cl, 0.1% (w/v) KH_2PO_4, 0.3% (w/v) K_2HPO_4, 0.05% (w/v) $MgSO_4$, 0.001% (w/v) $FeSO_4$, 0.1% (w/v) yeast extract, 1% (w/v) 1-tetradecanol, and 0.1% (w/v) Triton X-100. The culture medium was incubated aerobically with shaking (300 strokes/min) at 28°C for 24–48 h. Next, an aliquot (20–50 µL) of the medium, in which microorganism growth was observed, was transferred to a 3 mL fresh enrichment medium and incubated by shaking (300 strokes/min) at 28°C for another 24–48 h. Finally, an aliquot (10 µL) of the medium containing microorganisms was streaked onto a 2% (w/v) agar plate with the same composition as the isolation medium and cultivated at 28°C for 24–48 h. Following cultivation, single colonies on the agar plate were isolated and used for subsequent experiments.

Screening of microorganisms isolated from soil samples

The 1-tetradecanol-assimilating microorganisms were inoculated into a 10 mL isolation medium and cultivated at 28°C for 48 h. After cultivation, the cells were collected by centrifugation at room temperature at 1,500 × *g* for 10 min and added to a 1 mL reaction mixture consisting of 10 mM 1-tetradecanol, 5 mM NAD^+, 5 mM $NADP^+$, 1% (w/v) Triton X-100 in 100 mM Tris-HCl buffer (pH 8.5). The reaction mixture was incubated with shaking (300 strokes/min) at 28°C for 24 h. After the reaction,

the mixture was acidified with 5 N HCl, extracted with 1 mL toluene containing 1 mM 1-pentadecanol as an internal standard, and subjected to GC and GC-MS analyses.

GC and GC-MS analysis

The GC analysis was conducted using a Shimadzu GC-2010 Plus gas chromatograph (Shimadzu, Kyoto, Japan) equipped with a flame ionization detector and a Nukol capillary column (30 m × 0.25 mm × 0.25 μm; Supelco, Bellefonte, PA, USA). Helium at a flow rate of 1.12 ml/min was used as the carrier gas. Samples were injected with a split ratio of 50:1. The injector and detector were operated at 200°C. The heating program of the column consisted of the following steps: the initial column temperature of 80°C was raised to 112°C at a rate of 5°C/min, then raised to 190°C at a rate of 40°C/min, and held at 190°C for 45 min. The GC-MS was conducted using a Shimadzu GC-MS QP2010 (Shimadzu, Kyoto, Japan) equipped with a Nukol capillary column (30 m × 0.25 mm × 0.25 μm; Supelco) to identify the structure of products produced by microbial strains. The flow rate and the heating program were the same as those described above. A mass spectrometer was operated in the electron impact mode at 70 eV, with an ion source temperature of 200°C. Quantification was conducted by comparing peak areas with those from standard compounds.

Identification of selected strains via 16S rRNA sequence

Genomic DNA of a selected bacterial strain was extracted with DNeasy Blood & Tissue Kit (QIAGEN, Hilden, Germany) and used as the template for PCR. The gene encoding 16S rRNA sequence was amplified using PCR with the primer 1492R, 1100R, 802R, and 341F listed in Table S1.2. The PCR was performed using KOD-Plus-Neo DNA polymerase (Toyobo, Osaka, Japan) under the following reaction conditions: 94°C for 2 min and 30 cycles of 98°C for 10 s, 55°C for 30 s, and 68°C for an appropriate time (30 s/kb). The PCR products were purified using the QIAquick Gel Extraction Kit (Qiagen) and subjected to genetic analysis using the GenomeLab DTCS Quick Start kit and a Beckman Coulter CEQ8000 analyzer (Beckman Coulter, Brea, CA, USA).

Purification of the alcohol-oxidizing enzyme from *Pantoea* sp. 7-4

All protein purification processes in this study were conducted at 0°C–5°C using the AKTA pure chromatography system (GE Healthcare, Chicago, IL, USA). The activity of all protein fractions was measured using the spectrophotometric method mentioned in the next section, and all active fractions were subjected to SDS-PAGE analysis. First, cell pellets of *Pantoea* sp. 7-4 were suspended in 20 mM KPB, pH 7.0, and disrupted with an Insonator 201M ultrasonic oscillator (KUBOTA, Tokyo, Japan) for 5 min × 6 cycles followed by centrifugation at 12,000 × *g* for 20 min and ultracentrifugation at 100,000

× *g* for 60 min. The supernatant was recovered as a soluble protein fraction and was mixed with an equal volume of 20 mM KPB, pH 7.0, with 3 M ammonium sulfate. After mixing and centrifuging at 6,500 g for 20 min, the supernatant was recovered and subjected to a series of chromatography. Protein was purified using hydrophobic interaction chromatography in a HiTrap Phenyl HP 5 mL column (GE Healthcare), and eluted with 10 column volume (CV) of 20 mM KPB, pH 7.0. The active protein fractions were desalted and further purified via gel filtration chromatography in a Superdex 200 Increase 100/300 GL column (GE Healthcare), eluted with 1.3 CV of 20 mM KPB, pH 7.0, followed by anion exchange chromatography in a Q sepharose XL 1 mL column (GE Healthcare) with a NaCl linear gradient (0–1 M in 20 CV) in 20 mM KPB, pH 7.0.

The determination of enzyme activity

Enzyme activity was determined by measuring the absorbance change at 340 nm, which represented the NAD(P)H generated from $NAD(P)^+$ during the dehydrogenation reaction catalyzed by alcohol dehydrogenase. The reaction mixture (1 mL) consisted of 100 mM Tris-HCl (pH 8.5), 1 mM 1-tetradecanol, 3 mM NAD^+, 3 mM $NADP^+$, 0.01% (w/v) Triton X-100, and 10 µL enzyme fraction. The reaction components were mixed in a cuvette and pre-incubated at 25°C for 3 min before adding the substrate 1-tetradecanol. After adding the substrate, the absorbance at 340 nm of the reaction mixture was measured.

Protein analysis

The protein concentration was determined using a Bradford protein assay with a Bio-Rad Protein Assay kit (Bio-Rad Laboratories, Inc., Hercules, CA, USA). The SDS-PAGE was conducted on a 12.5% polyacrylamide gel with a Tris-glycine buffer system. Protein bands were stained using Coomassie Brilliant Blue R250. Protein bands were cut from the gel and transferred onto a PVDF membrane for sequencing. The NH_2-terminal amino sequence of the target protein was determined using automated Edman degradation with a PPSQ-31A protein sequencer (Shimadzu, Kyoto, Japan).

Cloning and expression of recombinant alcohol dehydrogenase PsADH

The *PsADH* gene (DDBJ accession number LC727629, Table S1.1) was amplified via PCR using the genomic DNA of the *Pantoea* sp. 7-4 strain as a template and the primer listed in Table S1.2. The PCR was performed using PrimeSTAR MAX DNA polymerase (Takara Bio, Shiga, Japan) under the following reaction conditions: 94°C for 2 min and 35 cycles of 98°C for 10 s, 55°C for 5 s, and 72°C for 1.5 min. The PCR product was mixed with the pET-21b(+) vector, which was digested with NotI and SalI and ligated using ClonTech Ligation Mix (Takara Bio), resulting in the plasmid pET-21b(+)-

PsADH. The plasmid was then transformed into *E. coli* competent cells. The *E. coli* DH5α was used as the cloning host and *E. coli* Rosetta 2 (DE3) was used as the expression host. The resulting strain *E. coli* Rosetta 2 (DE3)/pET-21b(+)-*PsADH* was inoculated into an LB medium containing ampicillin and chloramphenicol and cultivated at 37°C with shaking. When the optical density at 600 nm reached 0.8, culture was induced with 1 mM IPTG and cultivated at 16°C for 16 h with shaking. Protein expression was monitored by SDS-PAGE. After cultivation, cells were harvested via centrifugation, washed with 0.85% NaCl solution, and stored at −20°C for further use.

The purification of recombinant PsADH

For the purification of recombinant PsADH, cells of *E. coli* Rosetta 2 (DE3)/pET21b(+)-*PsADH* induced with IPTG were disrupted using the method mentioned in the previous section. Recombinant PsADH was then purified via anion exchange chromatography in a Q sepharose XL (1 mL) column with a NaCl linear gradient (0–1 M in 20 CV) in 20 mM KPB, pH 7.0, followed by gel filtration chromatography in a Superdex 200 Increase 100/300 GL column, eluted with 1.3 CV of 20 mM KPB, pH 7.0. The native molecular weight of PsADH was determined via gel filtration chromatography using Gel Filtration Calibration Kits (LMW and HMW; GE Healthcare).

The effect of electron acceptor

The effect of NAD^+ and $NADP^+$ on the purified PsADH was evaluated by measuring the absorbance change at 340 nm. The reaction mixture (1 mL), which consisted of 100 mM Tris-HCl buffer (pH 8.5), 0.5 mM 1-tetradecanol, 1 mM NAD^+ or $NADP^+$, 0.1% (w/v) Triton X-100, and 3.0 μg purified PsADH, was incubated at 25°C, and the absorbance at 340 nm was measured. The amount of NAD(P)H generated was calculated using its molar extinction coefficient (6.22 $mmol^{-1}l\ cm^{-1}$).

The effect of reaction pH

The pH-dependent enzyme assay was conducted for either dehydrogenation or reduction reaction catalyzed by purified PsADH. For the dehydrogenation reaction, the reaction mixture (1 mL) consisted of 0.5 mM 1-tetradecanol, 1 mM NAD^+, 0.1% (w/v) Triton X-100, and 3.0 μg purified PsADH in different types of buffer. For the reduction reaction, the mixture (1 mL) consisted of 0.5 mM tetradecanal, 1 mM NADH, 0.1% (w/v) Triton X-100, and 3.0 μg purified PsADH in different kinds of buffer. The buffers used were all in a concentration of 100 mM with detailed pH as follows: sodium acetate buffer (pH 5.0–5.5), KPB (pH 6.0–8.0), Tris-HCl buffer (pH 7.5–9.0), and sodium carbonate buffer (pH 9.0–10.0). The reaction mixture was incubated at 25°C and the absorbance at 340 nm was measured.

The effect of reaction temperature

The temperature-dependent enzyme assay was conducted for the dehydrogenation reaction catalyzed by purified PsADH. The reaction mixture (1 mL), which consisted of 100 mM Tris-HCl buffer (pH 9.0), 0.5 mM 1-tetradecanol, 1 mM NAD^+, 0.1% (w/v) Triton X-100, and 3.0 µg purified PsADH was incubated at different temperatures (20°C–60°C) for 10 min for each trial, and the absorbance at 340 nm was measured.

Thermal stability

The thermal stability of PsADH was evaluated for the dehydrogenation reaction. Before mixing with other reaction components, the purified PsADH was pre-incubated at different temperatures (20°C–70°C) for 1 h in 100 mM Tris-HCl buffer (pH 9.0) for each trial. The reaction mixture (1 mL) consisted of 100 mM Tris-HCl buffer (pH 9.0), 0.5 mM 1-tetradecanol, 1 mM NAD^+, 0.1% (w/v) Triton X-100, and 3.0 µg purified PsADH. After mixing, the reaction mixture was incubated at 25°C for 5 min, and the absorbance at 340 nm was measured.

Kinetic analysis

The kinetics parameters, including the Michaelis-Menten constant (K_M and k_{cat} values) against 1-tetradecanol (dehydrogenation reaction) or tetradecanal (reduction reaction), were calculated using the Hanes-Woolf plot. The molar extinction coefficient for NADH at 340 nm is 6.22 $mmol^{-1}\,l\,cm^{-1}$. For the dehydrogenation reaction, the mixture (1 mL) consisted of 100 mM Tris-HCl buffer (pH 9.0), 0.5 mM 1-tetradecanol, 0.5 mM NAD^+, 0.1% (w/v) Triton X-100, and 3.0 µg purified PsADH. For the reduction reaction, the mixture (1 mL) consisted of 100 mM KPB (pH 7.0), 0.5 mM tetradecanal, 0.24 mM NADH, 0.1% (w/v) Triton X-100, and 3.0 µg purified PsADH. After mixing, the reaction mixture was incubated at 25°C for 3 min and the absorbance at 340 nm was monitored.

Substrate specificity

The purified PsADH was reacted with alcohol substrates and the activity was determined by the amount of NADH generated, derived from the UV absorbance change at 340 nm. The reaction mixture (500 µL) consisted of 100 mM Tris-HCl at pH 9.0, 0.1 mM alcohol substrate, 1 mM NAD^+, 0.1% (w/v) Triton X-100, and 1 µg purified enzyme. The reaction components were mixed in a cuvette and pre-incubated at 25°C for 3 min before adding the alcohol substrate. After adding the substrate, the UV absorbance at 340 nm was monitored. The substrates tested were as follows: 1-hexanol, 1-octanol, 1-

decanol, 1-dodecanol, 1-tetradecanol, 1-hexadecanol, 1-octadecanol, oleyl alcohol, 2-dodecanol, and 7-tetradecanol.

RESULTS

Screening and identification of 1-tetradecanol-oxidizing microorganisms

A total of 350 microbial strains were isolated from the soil as 1-tetradecanol-assimilating microorganisms. Among them, 60 strains showed the ability to oxidize 1-tetradecanol, including 19 strains that produced tetradecanal, 27 strains that produced tetradecanoic acid, and 14 strains that produced both tetradecanal and tetradecanoic acid. Since the aim of this study was to find an enzyme that can generate tetradecanal for alkane production, strain 7-4 was chosen with the highest tetradecanal production among all strains. The tetradecanal produced by strain 7-4 was confirmed using gas chromatography-mass spectrometry (GC-MS; Figure S1.1 in the supplementary information), and the 16S rRNA sequence of strain 7-4 was found to exhibit 99% homology with that of *Pantoea* sp.. To further evaluate *Pantoea* sp. 7-4, a reaction using its cell-free extracts was conducted and it was revealed that that 1-tetradecanol was converted to tetradecanal only when NAD(P)$^+$ existed (Figure 1.1). Also, tetradecanal production remained at the same level when the reaction was performed under anaerobic condition. These results indicated that *Pantoea* sp. 7-4 might possess a dehydrogenase, requiring NAD(P)$^+$ as an electron acceptor, rather than an oxidase, which requires molecular oxygen as an electron acceptor.

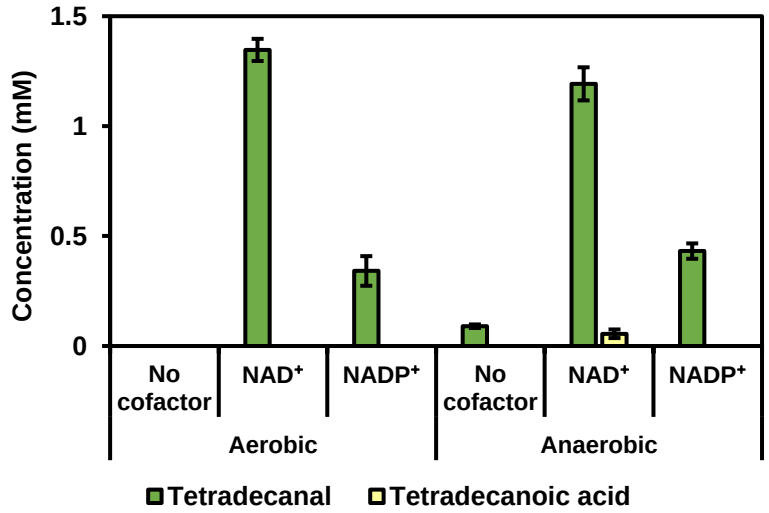

Figure 1.1 Effect of oxygen, NAD$^+$, or NADP$^+$ on the production of tetradecanal and tetradecanoic acid by *Pantoea* sp. 7-4. All experiments were performed in triplicate, and the data represent mean ± *SD* (*n* = 3).

Purification and identification of an alcohol dehydrogenase from *Pantoea* sp.

To identify the enzyme involved in the alcohol dehydrogenation reaction, the enzyme purification from the cell lysate of *Pantoea* sp. 7-4 was conducted via a fast protein liquid chromatography (FPLC) system and successfully purified an enzyme shown as a single protein band in Figure S1.2. The detailed

activity and yield during the purification process are shown in Table 1.1. The NH_2-terminal amino acid sequence of the purified protein was identified as follows:

MNMKIKTTMKAAVVKSFGEP

The above amino acid sequence was subjected to a BLAST search, and the result showed that it was 100% homologous with the sequence of an alcohol dehydrogenase from *Pantoea* sp. MSR2 (3). Based on these results, we named the purified enzyme, PsADH.

Table 1.1 Summary of the purification process of alcohol dehydrogenase from *Pantoea* sp. 7-4

Step	**Total protein (mg)**	**Total activity (U)**	**Specific activity (U/mg)**	**Yield (%)**	**Fold**
Cell-free extracts	511	162	0.32	100	1.00
Ammonium sulfate	347	145	0.42	89.0	1.31
HiTrap Phenyl HP	25.2	18.4	0.73	11.3	2.30
Superdex 200	3.89	8.68	2.23	5.30	7.02
Q sepharose XL	0.06	0.18	3.29	0.11	10.4

Cloning, expression, and purification of alcohol dehydrogenase PsADH

To elucidate the catalytic properties of PsADH, the *PsADH* gene was cloned from the isolated *Pantoea* sp. 7-4 strain into the pet-21b(+) vector and transformed it into *E. coli* Rosetta 2 (DE3). The cell lysate of IPTG-induced *E. coli* was then subjected to a series of column chromatography using an FPLC system, and the recombinant PsADH was purified (Figure S1.3). The purified enzyme was used for further characterization.

Characterization of recombinant PsADH

First, the effect of the cofactors was evaluated in the alcohol-oxidizing reaction using purified recombinant PsADH (Figure 1.2a). This revealed that PsADH catalyzed the reaction when beta-nicotinamide adenine dinucleotide, oxidized (NAD^+) was added but not when beta-nicotinamide adenine dinucleotide phosphate, oxidized ($NADP^+$) was added. Based on this result, it was assumed that PsADH is NAD^+-dependent alcohol dehydrogenase. Next, the optimal reaction pH of PsADH was evaluated for both dehydrogenation and reduction reactions (Figure 1.2b). The PsADH showed its highest activity at pH 9.0 with Tris-HCl buffer when catalyzing a dehydrogenation reaction, while its

highest activity occurred at pH 7.0 with KPB when catalyzing a reduction reaction. Furthermore, the optimal reaction temperature and the thermal stability of PsADH were evaluated for the dehydrogenation reaction. The PsADH showed the highest activity when it catalyzed the reaction at 40°C (Figure 1.2c). For thermal stability, the result showed that PsADH retained 90% of its original activity when incubated at temperatures between 20°C and 50°C, while its activity dropped to <20% when incubated at 60°C (Figure 1.2d). Finally, a kinetic analysis of PsADH was conducted using either 1-tetradenacol with NAD^+ as the substrate (dehydrogenation reaction) or tetradecanal with NADH as the substrate (reduction reaction; Table 1.2). The PsADH follows the Michaelis-Menten type reaction mechanism, where its k_{cat}/K_M values toward dehydrogenation and reduction reactions were 171 $s^{-1}\cdot mM^{-1}$ and 586 $s^{-1}\cdot mM^{-1}$, respectively.

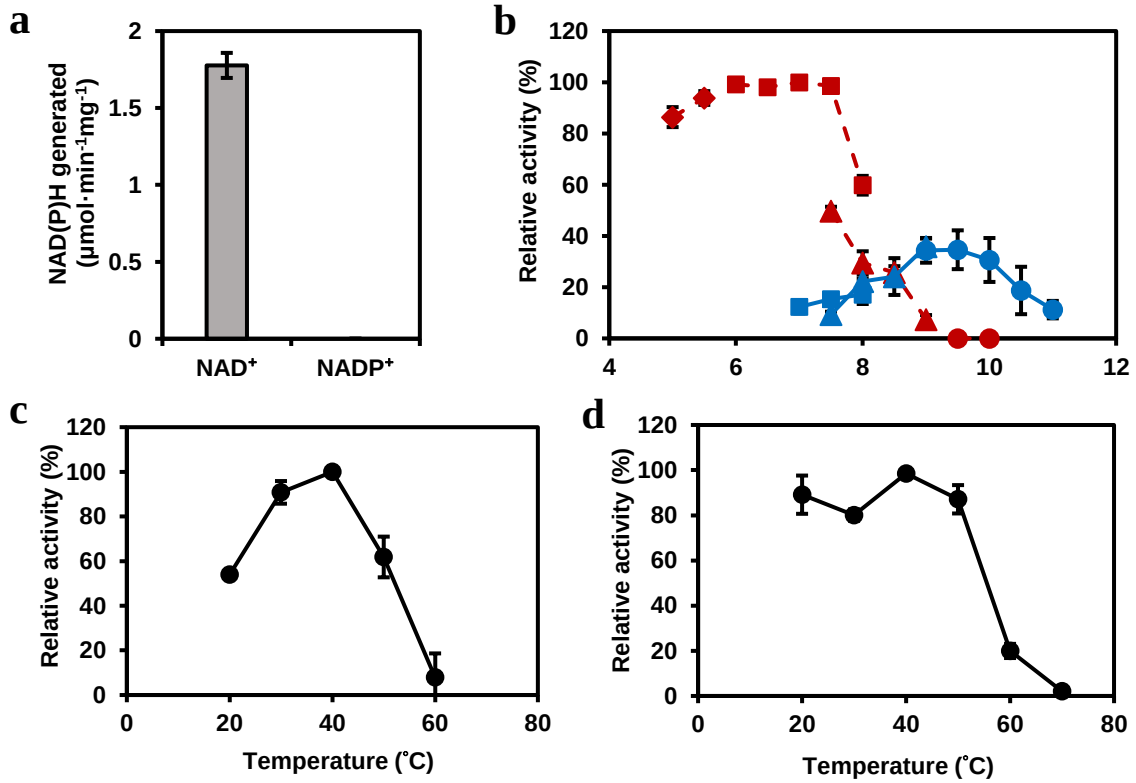

Figure 1.2 Characterization of recombinant PsADH. (a) Effect of cofactors for dehydrogenation reaction catalyzed by PsADH. (b) Effect of reaction pH. The blue lines indicate the dehydrogenation reaction, and the red lines indicate the reduction reaction. Diamond, sodium acetate buffer; square, potassium phosphate buffer; triangle, Tris-HCl buffer; and circle, sodium carbonate buffer. The activity of PsADH when catalyzing dehydrogenation reaction under pH 7.0 (potassium phosphate buffer) was defined as 100%. (c) Effect of reaction temperature and (d) thermal stability of PsADH for the dehydrogenation reaction. For (c) and (d), the activity of PsADH under 40°C was defined as 100%. All experiments were performed in triplicate, and the data represent mean ± *SD* (n = 3).

Table 1.2 Kinetic constants for the dehydrogenation of 1-tetradecanol and the reduction of tetradecanal by PsADH

Substrate	K_M (mM)	k_{cat} (s^{-1})	k_{cat}/K_M ($s^{-1}\cdot mM^{-1}$)
1-Tetradecanol	0.168	28.7	171
NAD^+	0.352	91.5	260
Tetradecanal	0.129	75.6	586
NADH	0.030	67.3	2240

Substrate specificity of alcohol dehydrogenase PsADH

The substrate specificity of PsADH toward fatty alcohols was investigated using the purified enzyme. First, alcohols ranging from short-chain (C6) to long-chain (C18) were chosen since their corresponding alkane products fit the carbon length of alkanes found in fossil fuels. The result indicated that PsADH had higher activity toward alcohols with shorter chain length such as 1-hexanol and 1-octanol (Figure 1.3). Additionally, the experiments were performed using secondary alcohols or unsaturated fatty alcohols. As a result, it was found that PsADH also showed activity toward 2-dodecanol, 7-tetradecanol, and oleyl alcohol.

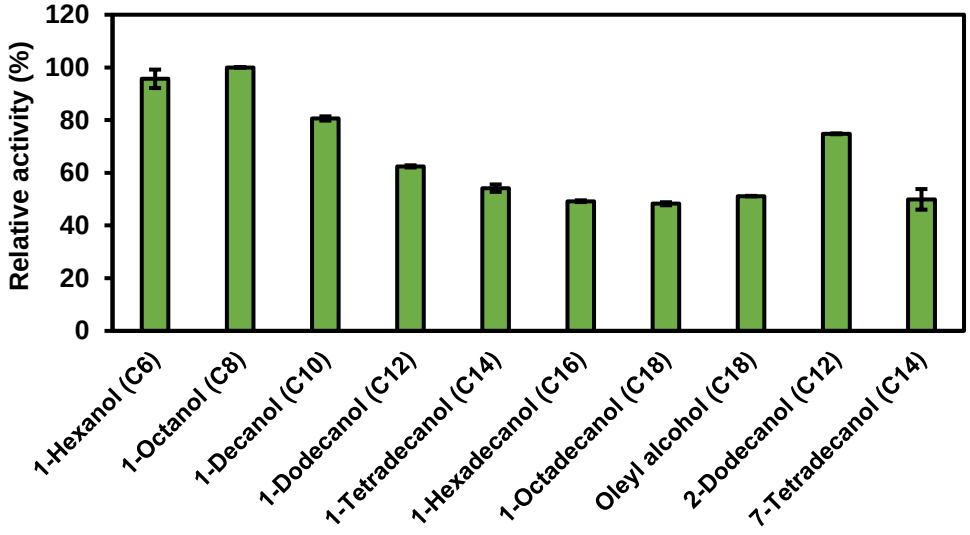

Figure 1.3 Substrate specificity of purified PsADH. The activity of PsADH when catalyzing the dehydrogenation of 1-octanol was defined as 100% (an absorbance change of 0.414 at 340 nm). All experiments were performed in triplicate, and the data represent mean ± *SD* (*n* = 3).

DISCUSSION

This study aims to develop a novel pathway to utilize alcohol byproducts generated in *E. coli* cells during alkane biosynthesis. The concept is to couple an aldehyde-oxidizing enzyme with ADO where fatty alcohols can be re-oxidized to fatty aldehydes for generating alkanes. Various enzymes found in nature perform alcohol oxidation; however, limited information has been reported regarding their activity toward medium-chain fatty alcohols (4–8). Therefore, a screening of 1-tetradecanol-assimilating microorganisms was conducted. The 1-tetradecanol has a carbon length of 14. Its corresponding product, tetradecanal, is a substrate favored by cyanobacterial ADOs to generate alkanes (9). As a result, the *Pantoea* sp. 7-4 strain was discovered as a good candidate since it produced the highest amount of tetradecanal among all strains screened. During the screening, other positive strains were also found to utilize 1-tetradecanol. For example, a *Pseudomonas* sp. 1-2 strain showed the ability to convert 1-tetradecanol to a relatively high amount of both tetradecanal and tetradecanoic acid (data not shown). However, since fatty acid is the undesired substrate for ADO in the downstream alkane biosynthetic process, *Pantoea* sp. 7-4 was chosen for further analysis.

Observed throughout nature, enzymes that perform alcohol oxidation can be divided into two groups, the alcohol dehydrogenase group [EC. 1.1.1] and the alcohol oxidase group [EC. 1.1.3]. An alcohol dehydrogenase normally requires $NAD(P)^+$ or FAD as an electron acceptor, whereas an alcohol oxidase requires molecular oxygen as an electron acceptor (3, 10). The initial results in this study indicated that *Pantoea* sp. 7-4 might possess a dehydrogenase (Figure 1.1). Subsequent sequence analysis of the enzyme PsADH purified from this strain also revealed that it belongs to the medium-chain dehydrogenases/reductases (MDR) family. The enzymes in this superfamily were reported to have a size of around 350 residues (molecular weight 38,500) and function as dimers or tetramers (11, 12). Interestingly, when the molecular weight of PsADH was conducted estimation, the result from gel filtration chromatography indicated its molecular weight to be 296,000 (Figure S1.4), while the result from SDS-PAGE as well as its sequence information indicated 36,800 (Figure S1.2 and Table S1.1). Considering the denaturation process during SDS-PAGE, PsADH was assumed to function as an octamer, which is an unusual character in the MDR superfamily.

To evaluate the synergy between PsADH and ADO, a series of biochemical parameters of PsADH were characterized using its recombinant protein. Kinetic analysis of PsADH (Table 1.2) showed a higher k_{cat}/K_M toward the reduction reaction (aldehyde to alcohol) than the dehydrogenation reaction (alcohol to aldehyde), a result also found in many alcohol dehydrogenases where short-chain alcohols were used as substrates (4–8). Thus, it will be important to maintain the concentration of substrate and cofactor in the cell when applying this enzyme to alkane production. Conversely, PsADH was found to

be an NAD^+-dependent alcohol dehydrogenase, based on our results (Figure 1.2a), making PsADH a suitable enzyme to be coupled with ADOs. It has been reported that the reaction catalyzed by cyanobacterial ADO requires oxygen as the cofactor and a reducing system consisting of ferredoxin, ferredoxin reductase, and NADPH, which provides four electrons per turnover (9, 13–17). PsADH needs neither oxygen nor $NADP^+$ to catalyze alcohol dehydrogenation. In the reduction of aldehyde, PsADH uses NADH but not NADPH. Based on these cofactor preferences, there will be no competition among these cofactors when PsADH is combined with ADO for alkane production.

An ADH with a broad substrate spectrum would be favored since the petroleum-based fuels currently used are composed of alkanes and alkenes ranging from short to medium (C8–C16) chain. However, studies on these enzymes mainly focused on their activities toward short-chain alcohols (4–8). In contrast, it has been reported that the product during fermentative production of alkane by the *E. coli* expressing cyanobacterial AR and ADO are C13–C17 alkanes or alkenes (9). Regarding the cleavage of terminal carbonyl moiety catalyzed by ADO (13–17), it is assumed that the precursor of alkane in such system would be C14–C18 fatty aldehyde. Thus an ADH with ability to generate medium chain aldehyde will be the key to link the alcohol dehydrogenation and the aldehyde deformylation reaction.

Here, for investigating the substrate specificity of PsADH, the reaction using purified recombinant PsADH with different alcohol substrates was conducted. The results in Figure 1.3 showed that PsADH had a broad substrate spectrum, where alcohols ranging from C6–C18 could be oxidized by PsADH. Surprisingly, the activity was also observed when the substrate was changed to oleyl alcohol, 2-dodecanol, and 7-tetradecanol. These findings suggested that PsADH could oxidize not only primary alcohols but also secondary alcohols or unsaturated alcohols. Such character made PsADH a useful enzyme when being applied to any reaction involving aldehyde formation, besides the production of bio-alkane. Moreover, the results revealed that PsADH can provide downstream alkane biosynthesis with aldehydes with suitable chain length.

The petroleum-based fuels currently used are composed of alkanes and alkenes ranging from short to medium (C8–C16) chain. Unfortunately, there has been limited information on ADOs with substrate specificity toward chain length less than C14. Besides, those well-studied cyanobacterial ADOs have shown a low turnover rate when catalyzing decarbonylation reactions (13–17). To improve the alkane titer to a competitive level with other biofuels, such as bioethanol (18), an enzyme with better alkane-producing activity is required.

Nevertheless, the work demonstrate in this chapter reveals a new possibility to reuse alcohol byproducts for alkane production. PsADH is found to be a NAD^+-dependent alcohol dehydrogenase which does not require oxygen to catalyze the alcohol-oxidizing reaction. Also the broad substrate

specificity of PsADH made it stand out of other alcohol dehydrogenases reported to date. These characters will provide PsADH with a great potential to be coupled with ADOs and other enzymes when constructing alkane biosynthetic pathways.

SUMMARY

Alkanes produced by microorganisms are expected to be an alternative energy source to fossil fuels. Microbial synthesis of alkanes involves the formation of fatty aldehydes via fatty acyl-CoA intermediates derived from fatty acid metabolism, followed by aldehyde decarbonylation to generate alkanes. Advancements in metabolic engineering have enabled the construction of such pathways in various microorganisms, including *Escherichia coli*. However, endogenous aldehyde reductases in the host microorganisms are highly active in converting fatty aldehydes to fatty alcohols, limiting the substrate pool for alkane production. To reuse the alcohol byproduct, a screening of fatty alcohol-assimilating microorganisms was conducted in this chapter. A bacterial strain, *Pantoea* sp. 7-4, was found to convert 1-tetradecanol to tetradecanal. From this strain, an alcohol dehydrogenase, PsADH, was purified and found to be involved in 1-tetradecanol-oxidizing reaction. Subsequent heterologous expression of the *PsADH* gene in *E. coli* was conducted, and recombinant PsADH was purified for a series of biochemical characterizations, including cofactors, optimal reaction conditions, kinetic parameters, and substrate specificity.

REFERENCES

1. J. M. Perez, F. A. Arenas, G. A. Pradenas, J. M. Sandoval, C. C. Vasquez. *Escherichia coli* YqhD exhibits aldehyde reductase activity and protects from the harmful effect of lipid peroxidation-derived aldehydes. *J. Biol. Chem.* **283**:7346–7353 (2008).
2. Z. Fatma, K. Jawed, A. J. Mattam, S. S. Yazdani. Identification of long chain specific aldehyde reductase and its use in enhanced fatty alcohol production in *E. coli*. *Metab. Eng.* **37**:35–45 (2016).
3. F. X. Nascimento, A. G. Hernandez, B.R. Glick, M. J. Rossi. The extreme plant-growth-promoting properties of *Pantoea phytobeneficialis* MSR2 revealed by functional and genomic analysis. *Environ. Microbiol.* **22**:1341–1355 (2020).
4. C. W. Bradshaw, H. Fu, G. J. Shen, C. H. Wong. A *Pseudomonas* sp. alcohol dehydrogenase with broad substrate specificity and unusual stereospecificity for organic synthesis. *J. Org. Chem.* **57**:1526–1532 (1992).
5. B. Machielsen, A. R. Uria, S. W. M. Kengen, J. van der Oost. Production and characterization of a thermostable alcohol dehydrogenase that belongs to the aldo-keto reductase superfamily. *Appl. Environ. Microbiol.* **72**:233–238 (2006).
6. P. Koutsompogeras, A. Kyriacou, I. Zabetakis. Characterizing NAD-dependent alcohol dehydrogenase enzymes of *Methylobacterium extorquens* and strawberry (*Fragaria* × *ananassa* cv. Elsanta). *J. Agric. Food. Chem.* **54**:235–242 (2006).
7. Y. C. Park, K. Y. San, G. N. Bennett. Characterization of alcohol dehydrogenase 1 and 3 from *Neurospora crassa* FGSC2489. *Appl. Microbiol. Biotechnol*. **76**:349–356 (2007).
8. O. de Smidt, J. C. du Preez, J. Albertyn. The alcohol dehydrogenases of *Saccharomyces cerevisiae*: a comprehensive review. *FEMS Yeast. Res.* **8**:967–978 (2008).
9. A. Schirmer, M. A. Rude, X. Li, E. Popova, S. B. del Cardayre. Microbial biosynthesis of alkanes. *Science* **329**:559–562 (2010).
10. P. Goswami, S. S. R. Chinnadayyala, M. Chakraborty, A. K. Kumar, A. Kakoti. An overview on alcohol oxidases and their potential applications. *Appl. Microbiol. Biotechnol.* **97**:4259–4275 (2013).
11. B. Persson, J. Hedlund, H. Jornvall. Medium and short chain dehydrogenase reductase gene and protein families. *Cell. Mol. Life. Sci.* **65**:3879–3894 (2008).
12. M. Knoll, J. Pleiss. The medium-chain dehydrogenase/reductase engineering database: a systematic analysis of a diverse protein family to understand sequence–structure–function relationship. *Protein Sci.* **17**:1689–1697 (2008).

13. D. Das, B. E. Eser, J. Han, A. Sciore, E. N. G. Marsh. Oxygen-independent decarbonylation of aldehydes by cyanobacterial aldehyde decarbonylase: a new reaction of diiron enzymes. *Angew. Chem. Int. Ed.* **50**:7148–7152 (2011).
14. D. M. Warui, N. Li, H. Nørgaard, C. Krebs, J. M. J. Bollinger, S. J. Booker. Detection of formate, rather than carbon monoxide, as the stoichiometric coproduct in conversion of fatty aldehydes to alkanes by a cyanobacterial aldehyde decarbonylase. *J. Am. Chem. Soc.* **133**:3316–3319 (2011).
15. E. N. G. Marsh, M. W. Waugh. Aldehyde decarbonylases: enigmatic enzymes of hydrocarbon biosynthesis. *ACS Catal.* **3**:2515–2521 (2013).
16. C. Jia, M. Li, J. Li, J. Zhang, H. Zhang, P. Cao, X. Pan, X. Lu, W. Chang. Structural insights into the catalytic mechanism of aldehyde-deformylating oxygenases. *Protein Cell* **6**:55–67 (2015).
17. L. J. Rajakovich, H. Nørgaard, D. M. Warui, W. C. Chang, N. Li, S. J. Booker, C. Krebs, J. M. J. Bollinger, M. E. Pandelia. Rapid reduction of the diferric-peroxyhemiacetal intermediate in aldehyde-deformylating oxygenase by a cyanobacterial ferredoxin: evidence for a free-radical mechanism. *J. Am. Chem. Soc.* **137**:11695–11709 (2015).
18. Y. Xu, J. Li, M. Zhang, D. Wang. Modified simultaneous saccharification and fermentation to enhance bioethanol titers and yields. *Fuel* **215**:647–654 (2018).

SUPPLEMENTARY INFORMATION

Table S1.1 Nucleotide sequence of *PsADH*

>PsADH

ATGAACATGAAGATCAAAACCACGATGAAAGCGGCAGTTGTGAAATCGTTCGGTGAGCCT
TTGGTGATTGAAGAAGTACCGGTGCCTTCGGTCGGGCCGGGTCAGGTTTTGGTAAAAATT
GCCGCCACCGGGGTTTGCCATACCGATTTGCACGCTGCTGAAGGTGACTGGCCGATCAAA
CCTAATCCCCCCTTTATTCCCGGCCATGAAGGTGTTGGTCAGGTTGTGGCGCTGGGCGAA
GGTGTGAAACATCTCAAACTTGGCGATCGCGTGGGTGTGCCCTGGCTCTACTCGGCCTGT
GGTCATTGCGAATATTGTCTCGATAGCTGGGAAACGCTGTGTCTGTCGCAGCAGAATGCC
GGTTATTCAGTCAATGGTAGCTTTGCAGAGTATTGCCTGGCGGATGCTAACTACGTCGGT
ATCCTGCCGGATAATATTGAGTATCATGAGATCGCACCGATTTTGTGTGCCGGTGTCACG
GTGTACAAAGGGCTGAAGATGACCGATACCAAGCCAGGTGACTGGGTGGTGATTTCCGGT
ATCGGTGGTTTGGGACATATGGCTGTTCAGTACGCGGTAGCGATGGGGCTTAACGTGGCT
GCTGTTGATATTGATGACGAGAAGCTGGAGTTTGCTAAACGTCTGGGTGCCAGCGTGGTG
GCTAACGCGAAAAATGTCGATCCGGCGAAATTCTTCCACGAAAGCTTCGGCGGCGCGCAC
GGTGTGCTGGTGACAGCGGTTTCACCGAAAGCCTTTGAGCAAGCGTTGGGAACCATGCGT
CGTGGCGGTACGATGGTGCTGAATGGCCTGCCGCCGGGCAAATTTGACCTGTCGATTTTT
GACATGGTGTTGGACGGTATTACGGTGCGCGGTTCAATTGTCGGCACCCGTAAGGATTTG
CAGGAGGCGCTCGACTTCGCTGGTCGTCACAAAGTGAAAGCCAATGTAGCGGTGGAGCCG
TTGGTCAACATCAACGATATCTTTGCCCGCATGCATGCCGGTAAAATTGAAGGCCGTATT
GTTGTTGATATGTCGCTGTAA

Table S1.2 Primers used in this chapter

Primers	Sequence
1492R	5′-GNTACCTTGTTACGACTT-3′
1100R	5′-AGGGTTGCGCTCGTTG-3′
802R	5′-TACCAGGGTATCTAATCC-3′
341F	5′-CCTACGGGNGGCWGCAG-3′
T7-F	5′-TAATACGACTCACTATAGGG-3′
T7-R	5′-TAGTTATTGCTCAGCGGTGG-3′
Adh-AS SalF	5′-GGGGTCGACATGAACATGAAGATCAAAACCACGATGAAAGCG-3′
Adh-AS NotR	5′-AAAGCGGCCGCTTACAGCGACATATCAACAACAATACGGCCTTC-3′
Adhseq1F	5′-ATGAAGGTGTTGGTCAGGTT-3′
Adhseq1R	5′-TTGCTCAAAGGCTTTCGGTG-3′

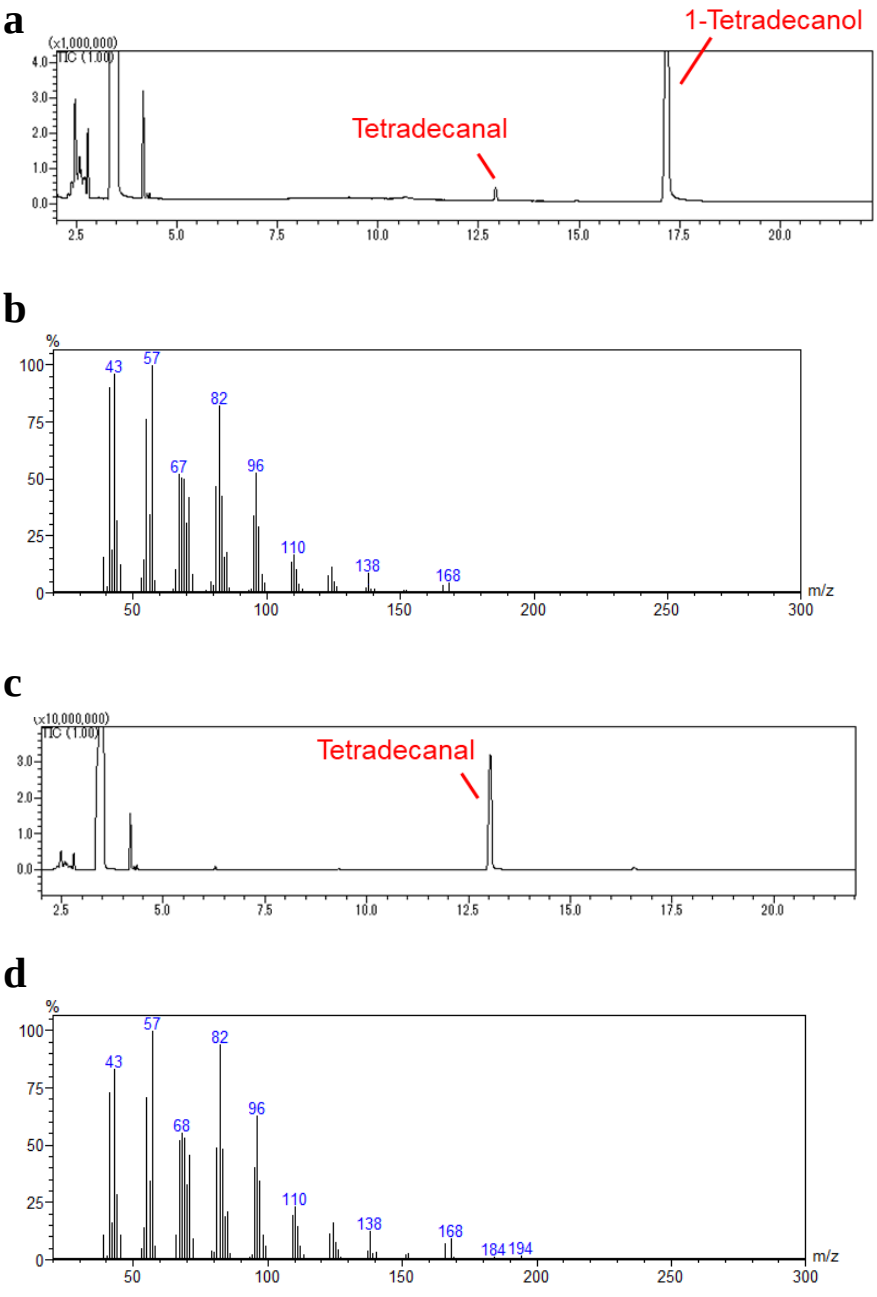

Figure S1.1 GC-MS analysis of tetradecanal.
(a) GC-MS total ion chromatogram of tetradecanal produced by strain 7-4.
(b) Mass spectrum of tetradecanal produced by strain 7-4.
(c) GC-MS total ion chromatogram of tetradecanal standard compound.
(d) Mass spectrum of tetradecanal standard compound.

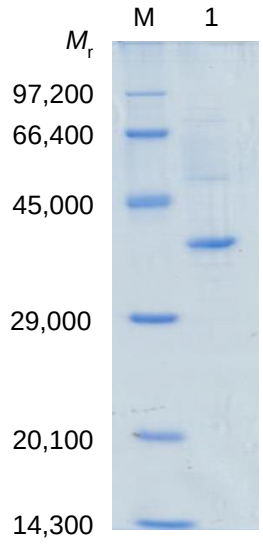

Figure S1.2 SDS-PAGE of protein fractions purified from *Pantoea* sp. 7-4. M, standard molecular weight. 1, single protein band of the 1-tetradecanol-oxidizing enzyme.

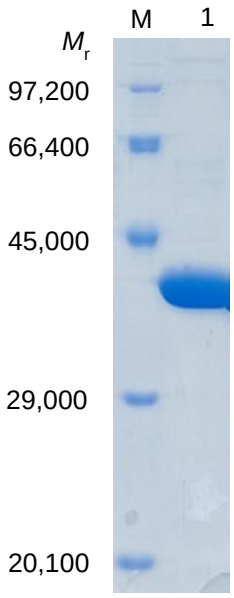

Figure S1.3 SDS-PAGE of protein fractions purified from *E. coli* Rosetta 2 (DE3)/pET21b-*PsADH*. M, standard molecular weight. 1, single protein band of recombinant PsADH.

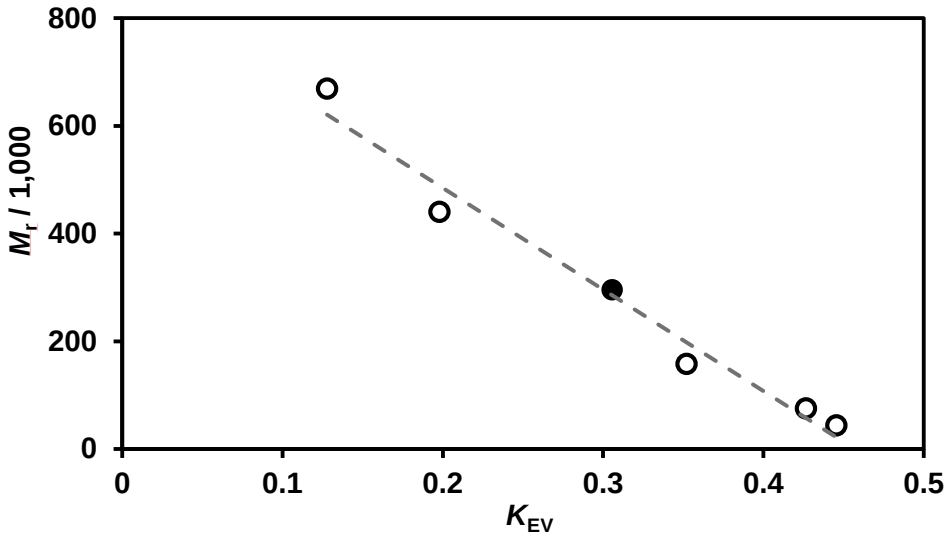

Figure S1.4 Calibration curve of protein molecular weight. White circles, molecular weight-elution volume constant plot of protein standards. Black circle, calculated molecular weight of PsADH based on its elution volume. Molecular weight of protein standards used are as follows: ovalbumin (44,000), conalbumin (75,000), aldolase (158,000), ferritin (440,000), and thyroglobulin (669,000).

CHAPTER 2

Utilizing alcohol for alkane production by introducing fatty alcohol dehydrogenase PsADH

INTRODUCTION

The dependence of fossil fuels has led to serious environmental problems in the world (1, 2). As an ideal alternative to fossil fuels, alkanes and alkenes produced by microorganisms have attracted great attention in recent years. These bio-based hydrocarbons are expected to better fit the engine infrastructures than other biofuels because their chemical compositions are relatively close to the petroleum-derived fuels (3). Microbial alkane synthesis involves the decarbonylation reaction of fatty aldehydes derived from fatty acid metabolism. For example, Schirmer *et al.*reported the biosynthesis of alkanes in engineered *Escherichia coli* by introducing the aldehyde-deformylating oxygenase (ADO) and the acyl-ACP reductase (AR) originated from cyanobacteria such as *Synechococcus elongatus* PCC7942 or *Nostoc punctiforme* PCC73102 (4). However, it was reported that the alkane production was strongly limited by the endogenous aldehyde reductases, which are active in reducing fatty aldehydes to fatty alcohols (5, 6). Regarding this issue, in the previous chapter, the screening of fatty alcohol-oxidizing microorganisms was conducted, and a fatty alcohol dehydrogenase, PsADH, was identified. This enzyme showed the activity to oxidize a variety of fatty alcohol into the corresponding fatty aldehydes. Such activity endows PsADH with the potential of regenerating intracellular fatty aldehydes for alkane production. Also, by combining PsADH with ADO, the direct production of alkane from alcohol could be achieved (Scheme 2.1).

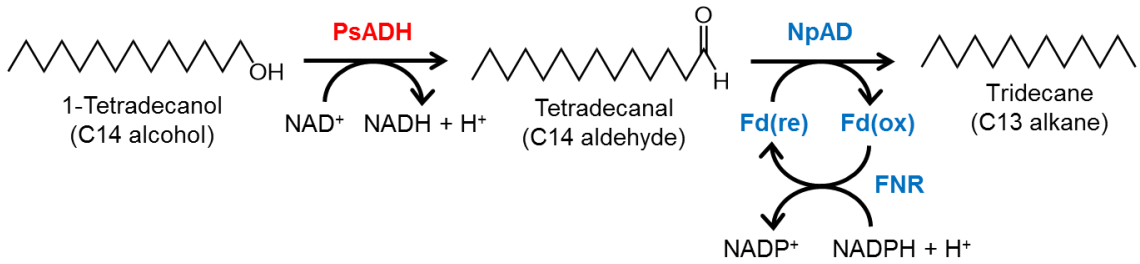

Scheme 2.1 Target reaction discussed in this chapter. PsADH, alcohol dehydrogenase. NpAD, aldehyde-deformylating oxygenase. Fd, ferredoxin. FNR, ferredoxin reductase.

It is reported that in the cyanobacteria *N. punctiforme* PCC73102, the aldehyde-deformylating oxygenase NpAD was found to catalyze the decarbonylation of fatty aldehydes along with a reducing enzyme system, including a ferredoxin (Fd) and a ferredoxin $NADP^+$-reductase (FNR), showing in blue color in Scheme 2.1. Here in this chapter, the co-expression of PsADH with NpAD, Fd, and FNR was carried out using *E. coli* as host to evaluate the feasibility of PsADH in alkane biosynthesis

Furthermore, to improve the efficiency of this system, the reaction conditions were optimized. The substrate specificity toward different alcohol substrates was also examined, demonstrating the potential of launching the alcohol-aldehyde-alkane synthetic route to the production of biofuels.

MATERIALS AND METHODS

Chemicals, microbial strains, nucleotide sequences, primers, and plasmids

Unless otherwise noted, chemicals were purchased from Fujifilm Wako Pure Chemical Corporation (Osaka, Japan). 1-Tetradecanol was purchased from Tokyo Chemical Industry Co., LTD. (Tokyo, Japan). Beta-nicotinamide adenine dinucleotide oxidized (NAD^+) disodium salt was purchased from Oriental Yeast Co., LTD. (Tokyo, Japan). *E. coli* DH5α and *E. coli* Rosetta 2 (DE3) (Merck, Darmstadt, Germany) was used as host for heterologous gene expression. Bacterial strain *Pantoea* sp. 7-4 was isolated from soil. The nucleotide sequences (Table S2.1) and the primers (Table S2.2) used in this chapter are shown in the supplementary information. The plasmid pET-21b (+), pRSFDuet-1 and pCDFDuet-1 (Merck) were used as the expression vectors.

Construction of *E. coli* strains for co-expression of PsADH, NpAD, Fd, and FNR

The methods of vector construction are the same as those described in previous chapter. Codon-optimized genes (Table S2.1) encoding the proteins of aldehyde deformylating oxygenase, ferredoxin, and ferredoxin $NADP^+$-reductase derived from *N. puntiforme* PCC73102 were synthesized and ligated into pRSFDuet-1 and pCDFDuet-1 vectors using the same method as described in previous section: NpAD (NCBI accession number WP_012408400), Fd (NCBI accession number WP_012408585), and FNR (NCBI accession number WP_012409282). The resulting plasmids were designated pRSF-*PsADH-NpAD* and pCDF-*Fd-FNR*, and were transformed into *E. coli* Rosetta 2 (DE3). The constructed *E. coli* strain were cultivated in LB medium with necessary antibiotics at 37°C with shaking. When the optical density at 600 nm reached 0.8, the culture was induced with 0.5 mM IPTG and cultivated at 16°C for 16 h with shaking. Protein expression was monitored by SDS-PAGE. After cultivation, the cells were harvested via centrifugation, washed with 0.85% NaCl solution, and stored at −20°C for further use.

Alkane productivity assay

Alkane production by *E. coli* Rosetta 2 (DE3)/pRSF-*PsADH-NpAD*/pCDF-*Fd-FNR* strain was evaluated using its resting cells. Another strain of *E. coli* Rosetta 2 (DE3)/pRSF-*NpAD*/pCDF-*Fd-FNR*, which does not harbor the *PsADH* gene, was used as the control. The reaction mixture (1 mL) consisted of 100 mM Tris-HCl buffer (pH 9.0), 2 mM 1-tetradecanol, 5 mM NAD^+, 5 mM NADPH, 0.1% (w/v) Triton X-100, and approximately 20 mg wet cell weights of induced *E. coli* cells. The reaction mixture was prepared in a 15 mL screw-capped test tube and incubated with shaking (120 strokes/min) at 40°C for 24 h. After the reaction, the mixture was acidified with 5 N HCl and extracted with 1 mL toluene

containing 1 mM 1-pentadecanol as the internal standard. The extracted sample was then subjected to GC and GC-MS to analyze the products.

Optimization of reaction pH and reaction temperature

The optimization of reaction pH and reaction temperature were conducted using the resting cell of *E. coli* Rosetta 2 (DE3)/pRSF-*PsADH-NpAD*/pCDF-*Fd-FNR* strain. The reaction mixture (1 mL) consisted of 100 mM buffer, 2 mM 1-tetradecanol, 5 mM NAD^+, 5 mM NADPH, 0.1% (w/v) Triton X-100, and 20 mg wet cell weights of induced *E. coli* cells. The reaction mixture was prepared in a 15 mL screw-capped test tube and incubated with shaking (120 strokes/min) for 24 h. For the optimization of reaction pH, the reaction buffers used are 100 mM potassium phosphate buffer (KPB) ranging from pH 6.0–8.0, and the reaction temperature was set at 30°C. For the optimization of reaction temperature, the reaction buffer used are 100 mM KPB at pH 7.5, and the reaction temperature was set at 20–50°C. After the reaction, the mixture was acidified with 5 N HCl and extracted with 1 mL toluene containing 1 mM 1-pentadecanol as the internal standard. The extracted sample was then subjected to GC and GC-MS to analyze the products.

GC and GC-MS analysis

The GC analysis was conducted using a Shimadzu GC-2010 Plus gas chromatograph (Shimadzu, Kyoto, Japan) equipped with a flame ionization detector and a Nukol capillary column (30 m × 0.25 mm × 0.25 μm; Supelco, Bellefonte, PA, USA). Helium at a flow rate of 1.12 ml/min was used as the carrier gas. Samples were injected with a split ratio of 50:1. The heating program of the column consisted of the following steps: the initial column temperature of 80°C was raised to 112°C at a rate of 5°C/min, then raised to 190°C at a rate of 40°C/min, and held at 190°C for 65 min. The GC-MS analysis was conducted using a Shimadzu GC-MS QP2010 (Shimadzu, Kyoto, Japan) with the same method described above. A mass spectrometer was operated in the electron impact mode at 70 eV, with an ion source temperature of 200°C. Note that only when analyzing the production of pentane and heptane, the heating program of the column was changed to the following steps to obtain a better separation: the initial column temperature of 60°C was raised to 112°C at a rate of 8°C/min, then raised to 190°C at a rate of 40°C/min, and held at 190°C for 65 min.

Time-course analysis of alkane production

The progress of alkane production by the *E. coli* cells expressing *PsADH-NpAD-Fd-FNR* was monitored through 0–48 h. The reaction mixture (1 mL) consisted of 100 mM KPB at pH 7.5, 2 mM 1-tetradecanol, 5 mM NAD^+, 5 mM NADPH, 0.1% (w/v) Triton X-100, and 20 mg wet cell weights of

induced *E. coli* cells. The reaction mixture was incubated at 30°C with shaking (120 strokes/min). The reaction mixture was extracted by the method mentioned in previous section, and the amount of 1-tetradecanol, tetradecanal, and tridecane at 0, 1, 2, 3, 6, 24, 48 h was analyzed by GC.

Assay of cell amount effects

The effects of cell amount were evaluated by using the resting cell of *E. coli* cells expressing *PsADH-NpAD-Fd-FNR*. The reaction mixture (1 mL) consisted of 100 mM KPB with pH 7.5, 2 mM 1-tetradecanol, 5 mM NAD^+, 5 mM NADPH, 0.1% (w/v) Triton X-100, and 20–80 g wet cell weights of induced *E. coli* cells. The reaction mixture was incubated at 30°C with shaking (120 strokes/min) for 24 h. The reaction mixture was extracted by the method mentioned in previous section, and the amount of 1-tetradecanol, tetradecanal, and tridecane at 0, 1, 2, 3, 6, 24, 48 h was analyzed by GC.

Substrate specificity assay of alkane-producing *E. coli*

The *E. coli* cells expressing *PsADH-NpAD-Fd-FNR* was reacted with different fatty alcohol substrates for evaluating the substrate specificity. The reaction mixture (1 mL) consisted of 100 mM KPB with pH 7.5, 2 mM alcohol substrate, 5 mM NAD^+, 5 mM NADPH, 0.1% (w/v) Triton X-100, and 20 g wet cell weights of induced *E. coli* cells. The substrates tested were as follows: 1-hexanol, 1-octanol, 1-decanol, 1-dodecanol, 1-tetradecanol, 1-hexadecanol, 1-octadecanol, and oleyl alcohol. The reaction mixture was incubated at 30°C with shaking (120 strokes/min) for 24 h. The reaction mixture was extracted by the method mentioned in previous section, and the alkane products generated by the cells were analyzed by GC and GC-MS. The product peaks were confirmed by comparing the GC-MS data with those of standard compounds (Hydrocarbon Mixture Standard, C9-C40 in n-Hexane) (GL Sciences Inc., Tokyo, Japan). Note that only when analyzing the production of nonane, the extraction was conducted using hexane instead of toluene since the peak of nonane was overlapped with the peak of toluene solvent under the conditions of GC and GC-MS analytical method used.

Substrate specificity assay using cell-free extracts of alkane-producing *E. coli*

The cell pellets of *E. coli* cells expressing *PsADH-NpAD-Fd-FNR* were suspended in 100 mM KPB with pH 7.5, and disrupted with an ultrasonic sonicator (Yamato Scientific Co., Tokyo, Japan) for 5 cycles, where each cycle contained 1 min of sonication and 1 min of rest. The cell disruption was operated at 0°C. The lysate was centrifuged at 12,000 × *g* for 20 min and the pellets were removed to obtain the cell-free extracts. The cell-free extracts were reacted with different fatty alcohol substrates for evaluating the substrate specificity. The reaction mixture (1 mL) consisted of 100 mM KPB with pH 7.5, 2 mM alcohol substrate, 5 mM NAD^+, 5 mM NADPH, 0.1% (w/v) Triton X-100, and cell-free

extracts obtained from 20 g wet cell weights of *E. coli* cells. The substrates tested were as follows: 1-tetradecanol, 1-hexadecanol, 1-octadecanol, and oleyl alcohol. The reaction mixture was incubated at 30°C with shaking (120 strokes/min) for 24 h. The reaction mixture was extracted by the method mentioned in previous section, and the alkane products were analyzed by GC.

RESULTS

Construction of *E. coli* expressing *PsADH-NpAD-Fd-FNR* and evaluation of its alkane production

To evaluate the potential use of PsADH in alkane production, the co-expression of PsADH with an ADO using *E. coli* as the host was carried out. NpAD, the ADO from cyanobacterium *N. punctiforme* PCC73102, as well as ferredoxin (Fd) and ferredoxin-$NADP^+$ reductase (FNR) from the same spices, was chosen as a system reported to convert aldehydes to alkanes. The expression of enzymes in the transformed *E. coli* strains was confirmed using SDS-PAGE (Figure S2.1), and the alkane production was analyzed using GC and GC-MS. The results of alkane productivity assay revealed that the *E. coli* strain harboring *NpAD-Fd-FNR* gene clusters produced no tridecane from 1-tetradecanol, whereas the strain harboring *PsADH-NpAD-Fd-FNR* gene clusters produced 0.15 mM tetradecanal and 0.12 mM tridecane from 2 mM 1-tetradecanol, under the reaction conditions used in Chapter 1 (Figure 2.1).

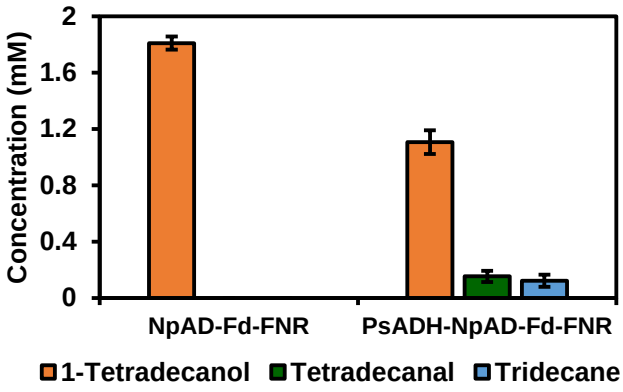

Figure 2.1 Alkane production of transformed *E. coli* strains. NpAD-Fd-FNR, *E. coli* strain expressing *NpAD*, *Fd*, and *FNR*; PsADH-NpAD-Fd-FNR, *E. coli* strain expressing *PsADH*, *NpAD*, *Fd*, and *FNR*. All experiments were performed in triplicate, and the data represent mean ± *SD* (*n* = 3).

Optimal reaction pH and temperature of *E. coli* expressing *PsADH-NpAD-Fd-FNR*

To improve the yield of alkane from fatty alcohol, the optimization of several reaction parameters using *E. coli* cells expressing *PsADH-NpAD-Fd-FNR* genes was conducted. First, the optimal reaction pH and reaction temperature were evaluated. For pH dependency, it was found that the highest alkane production occurred at pH 7.5 within the range of pH 6.0–8.0 (Figure 2.2). For temperature dependency, the experiments were conducted with different temperatures ranging from 20°C–50°C under pH 7.5. As a result, it was found that the cells produced the highest amount of alkane at 30°C (Figure 2.3).

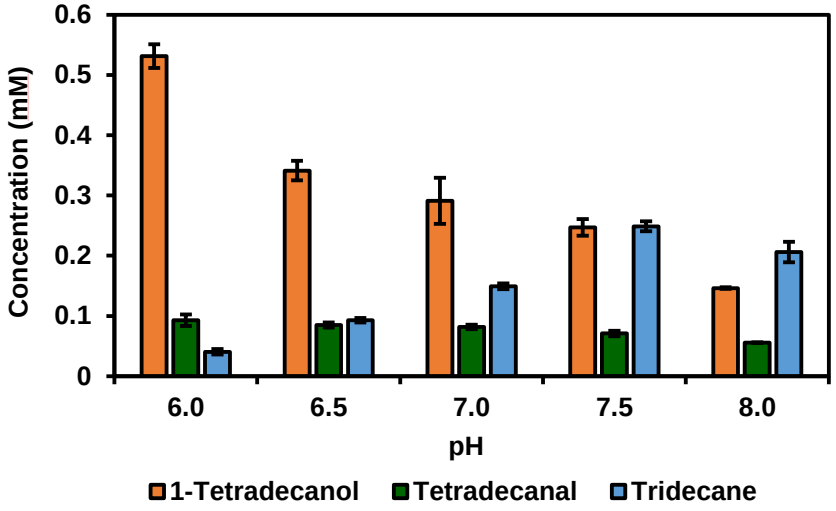

Figure 2.2 pH dependency of *E. coli* cells expressing *PsADH-NpAD-Fd-FNR*. All experiments were performed in triplicate, and the data represent mean ± *SD* (*n* = 3).

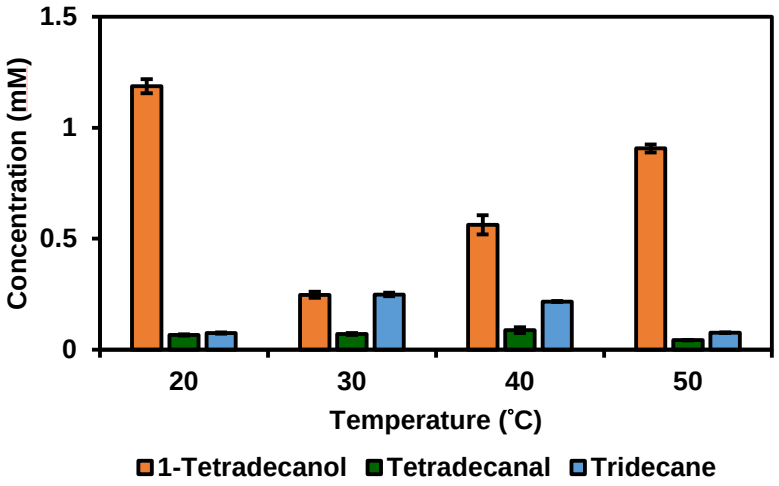

Figure 2.3 Temperature dependency of *E. coli* cells expressing *PsADH-NpAD-Fd-FNR*. All experiments were performed in triplicate, and the data represent mean ± *SD* (*n* = 3).

The time course of alkane production

To investigate the reaction progress in detail, the alkane-producing reaction from 0–48 h under the optimal reaction pH and temperature was monitored. According to the result shown in Figure 2.4, the alkane titer increased during 0–6 h, and remained at a constant level afterwards. In contrast, the substrate, 1-tetradecanol, decreased drastically during 0–6 h. The intermediate, tetradecanal, increased to the highest amount at 6 h and decreased afterwards.

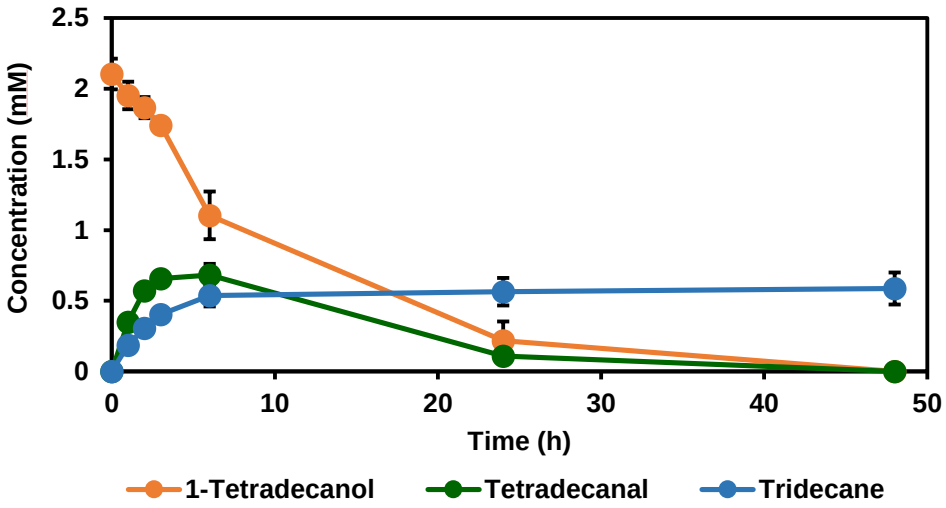

Figure 2.4 Time course of the substrate, intermediate and product during the reaction using *E. coli* cells expressing *PsADH-NpAD-Fd-FNR*. All experiments were performed in triplicate, and the data represent mean ± *SD* (*n* = 3).

Effects of cell amount

Next, the effects of existing amount of the enzyme in the reaction mixture were examined. This was done by adding various amount of cells to the reaction mixture. Alkane production with 20, 40, 60, and 80 mg of transformed *E. coli* cells was evaluated, and the result showed that the more the cells used, the higher the alkane production was (Figure 2.5). By applying 80 mg cells for the reaction, 1.03 mM of tridecane was produced from 2 mM 1-tetradecanol, with a 52% conversion rate.

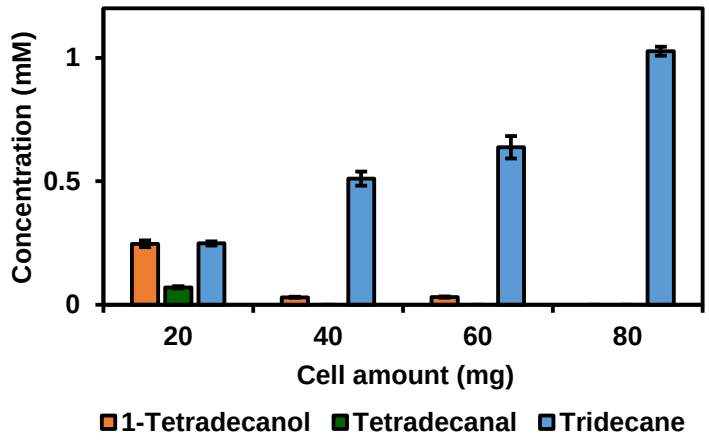

Figure 2.5 The effect of cell amount to the reaction using *E. coli* cells expressing *PsADH-NpAD-Fd-FNR*. All experiments were performed in triplicate, and the data represent mean ± *SD* (*n* = 3).

Substrate specificity of *E. coli* Rosetta2 (DE3)/pRSF-PsADH-NpAD-Fd-FNR.

Finally, the substrate specificity of the *E. coli* expressing *PsADH-NpAD-Fd-FNR* toward various fatty alcohols was investigated. This experiment included primary alcohols ranging from C6 to C18. The alkanes generated in the reaction mixture were confirmed by GC and GC-MS and shown in Figure S2.2 to Figure S2.9 in the supplementary information. Besides 1-tetradecanol, the *E. coli* strain also showed the ability to produce short-chain alkanes such as pentane and heptane from their corresponding alcohol substrates (Figure 2.6). On the other hand, the strain showed low activity toward 1-hexadecanol, and no activity toward 1-octadecanol and oleyl alcohol.

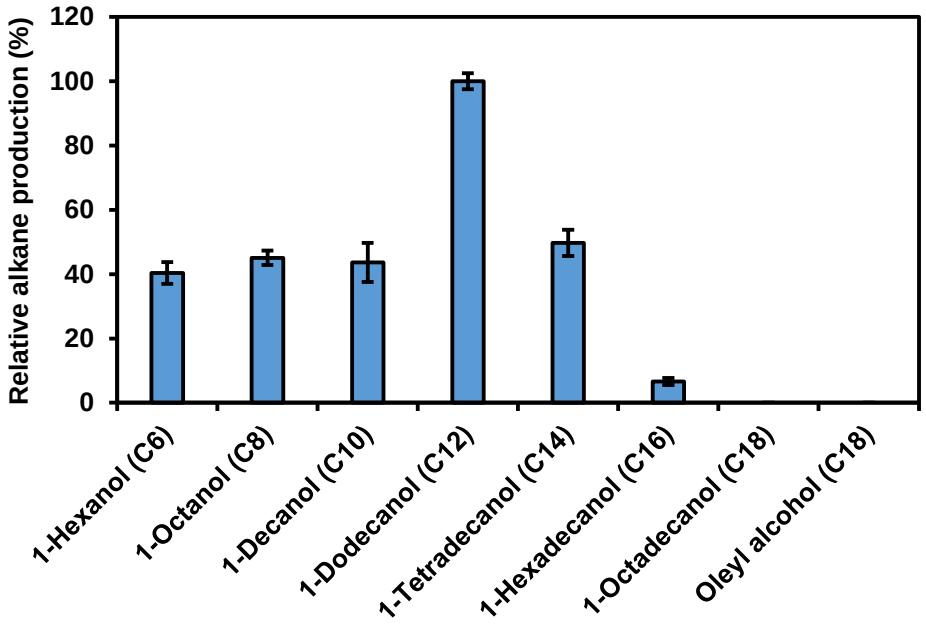

Figure 2.6 Substrate specificity of *E. coli* cells expressing *PsADH-NpAD-Fd-FNR*. Undecane production (0.43 mM) from 1-dodecanol was set as 100%. All experiments were performed in triplicate, and the data represent mean ± *SD* (n = 3).

DISCUSSION

To date, studies on the alcohol dehydrogenases mainly focused on their activities toward short-chain alcohols (alcohols with carbon length less than C8) (7–11). In contrast, the alcohols generated by endogenous aldehyde reductases in *E. coli* range from medium to long chain (C14 – C18) (6, 12, 13). To effectively utilize these fatty alcohols, an alcohol dehydrogenase with activity toward substrates with the desired chain length remained in need. In the previous chapter, a screening of microorganisms was carried out and an alcohol dehydrogenase PsADH, originated from a *Pantoea* sp. 7-4 strain isolated from soil, was discovered. This is an enzyme capable of oxidizing a wide range of fatty alcohols, including those found in alkane-producing *E. coli*.

In this chapter, the function of PsADH was further evaluated by co-expressing PsADH with NpAD, a cyanobacterial aldehyde-deformylating oxygenase, using *E. coli* as host. The result in Figure 2.1 showed that the *E. coli* expressing *PsADH-NpAD-Fd-FNR* genes successfully convert 1-tetradecanol to tetradecanal and tridecane, the first-reported direct production of alkane from alcohol. At first, the reaction conditions were set as the optimal conditions that suitable for PsADH, which were 40°C and pH 9.0 based on the results in Chapter 1. This resulted in a conversion rate of approximately 6%, with 0.12 mM tridecane being produced from 2 mM 1-tetradecanol (Figure 2.1). However, such conditions may not be suitable for NpAD. Since PsADH can catalyze alcohol-oxidizing reactions under a wide range of pH and temperature (Figure 1.2b–1.2d), it was assumed that the efficiency of this system can be improved by adjusting these parameters. Thus in the subsequent experiments, the reaction conditions for the constructed alkane-producing *E. coli* was re-evaluated.

The optimal reaction conditions of *E. coli* expressing *PsADH-NpAD-Fd-FNR* genes revealed that tridecane production from 1-tetradecanol was the highest under pH 7.5 and 30°C, shown in Figure 2.2 and 2.3. The results showed that the cells had greater activity under pH 7.5 and pH 8.0, indicating that an alkaline pH is favored for the reaction. In contrast, the results in previous chapter revealed that PsADH itself had the highest activity at pH 9.0 when catalyzing the dehydrogenation of 1-tetradecanol (Figure 1.2b). Yet there has been no study focusing on the optimal reaction conditions of NpAD, it was speculated that NpAD favors a neutral pH when catalyzing aldehyde-deformylating reaction based on the data in this study.

To determine the suitable reaction time, the time course of alkane-producing reaction was monitored. As shown in Figure 2.4, the amount of tridecane increased rapidly within 6 h and remained at a constant level afterwards. On the other hand, the amount of the substrate 1-tetradecanol showed a similar trend, where it decreased drastically within 6 h. The result indicated that 6 h would be a suitable reaction time, and that there may be factors limiting the alkane production. By considering the time

course of the intermediate, tetradecanal, it was assumed that a possible factor may be the deficiency of the cofactor for PsADH. A cofactor such as NAD^+ was necessary when PsADH catalyzed the oxidative reaction. However, NAD^+ were also consumed by other enzymes in the cells. Once NAD^+ was depleted, no more fatty aldehydes could be generated from PsADH for alkane production. To facilitate the reaction involving PsADH, a system which regenerates NAD^+ from NADH could be necessary.

As the last part of the optimization, the effect of the cell amount in the reaction was evaluated. The result in Figure 2.5 revealed that the alkane production was approximately proportional to the amount of cells applied to the reaction mixture. Overall, a 52% conversion of 1-tetradecanol to tridecane was achieved. The result pointed out that this system may help reuse the majority of alcohol byproducts generated during alkane production using engineered *E. coli*.

Furthermore, the substrate specificity of *E. coli* expressing *PsADH-NpAD-Fd-FNR* was evaluated (Figure 2.6). Alkanes ranging from C5 (pentane) to C15 (pentadecane) were produced successfully from their corresponding alcohol substrates. The cell revealed its highest activity when converting 1-dodecanol to undecane. For long-chain alcohols such as 1-hexadecanol, 1-octadecanol, and oleyl alcohol, however, the *E. coli* cells showed low or no production of alkanes. Considering that PsADH showed a wide substrate specificity including long-chain alcohols (Figure 1.3), and that heptadecane and heptadecene was reported to be produced by *E. coli* harboring NpAD using glucose as starting material (4), there may be other factors interfering the production of long chain alkanes from fatty alcohols.

To address this issue, increasing the cell permeability for these long-chain alcohol substrates turned out to be a possible solution. It was assumed that the low alkane production toward long-chain alcohols in Figure 2.6 resulted from the low solubility of the substrates. Unlike the alcohols generated inside the cells during alkane fermentation production, the alcohols used in the current experiments in Figure 2.6 was added extracellularly, leading to a low substrate availability for the enzyme. Thus, to help facilitate the reaction, the alkane productivity assay using the cell-free extracts of *E. coli* expressing *PsADH-NpAD-Fd-FNR* was carried out as an additional experiment showing in Figure S2.10 in supplementary information. In this experiment, the enzyme source was changed to the cell-free extracts instead of resting cells. By releasing the enzymes to the reaction mixture, the production of pentadecane, heptadecane, and heptadecene from their corresponding alcohol substrates were observed. Although the titer of these long-chain alkanes remained at a low level, this approach revealed that the access of the substrates to the enzymes plays an important role in this reaction system.

Another possible factor which may limit the alkane biosynthesis is the one-carbon moiety byproduct generated during the decarbonylation of aldehydes by ADO. To date, it was commonly agreed that for NpAD, the ADO from *N. punctiforme* PCC73102, the one-carbon moiety byproduct is

released as the form of formic acid (14). To further confirm the existence of formic acid in the reaction system reported in this study, an analysis of formic acid in aqueous solution was carried out by applying a reported method (15, 16). The result of LC-MS analysis indicated that, in the resting cell reaction catalyzing the conversion of 1-tetradecanol to tridecane, formic acid was indeed generated (data not shown). Although the reaction pH did not change much after the resting cell reaction since the reaction was performed in a buffer system, the formation of formic acid may still act as a factor to limit the enzyme activity. Besides, during the fermentative production of alkane, the accumulation of formic acid byproduct may decrease the pH of the medium and lead to a worse cell growth and lower alkane production. To improve the alkane production in microorganisms, solutions to these issues remained in need.

Taking all together, the work in this chapter demonstrated a novel synthetic pathway of alkanes using fatty alcohols as the starting material. The evaluation of substrate specificity and the optimization of reaction conditions revealed the necessary information when applying the alcohol dehydrogenase PsADH to alkane production. The high conversion rate of fatty alcohols to alkanes shown in this study suggested that the alcohol-aldehyde-alkane synthetic route could serve as an efficient way to reuse alcohol byproducts generated by *E. coli* endogenous aldehyde reductases.

SUMMARY

Hydrocarbons generated from microorganisms are expected to serve as the next-generation biofuel. Although many studies have demonstrated the biosynthesis of alkanes in microorganisms such as *E. coli*, the alkane production was strongly limited by the endogenous aldehyde reductases which transforms the important intermediate, fatty aldehydes, into fatty alcohols. In this chapter, by co-expressing the newly found alcohol dehydrogenase PsADH with an aldehyde-deformylating oxygenase NpAD, one-pot conversion of 1-tetradecanol to tridecane was achieved. Furthermore, by optimizing the reaction conditions, the conversion rate was increased to 52%. When conducting the reaction under conditions of pH 7.5 and 30°C with 80 mg *E. coli* cells expressing *PsADH-NpAD-Fd-FNR* genes, 1.03 mM tridecane was produced from 2 mM 1-tetradecanol. Besides, this system was found to be capable of producing alkanes ranging from C5–C17 with carbon length useful for serving as biofuels.

REFERENCES

1. J. H. Mercer. West Antarctic ice sheet and CO2 greenhouse effect: a threat of disaster. *Nature* **271**:321–325 (1978).
2. H. Rodhe. A comparison of the contribution of various gases to the greenhouse effect. *Science* **248**:1217–1219 (1990).
3. R. M. Lennen, D. J. Braden, R. M. West, J. A. Dumesic, B. F. Pfleger. A process for microbial hydrocarbon synthesis: overproduction of fatty acids in *Escherichia coli* and catalytic conversion to alkanes. *Biotechnol. Bioeng.* **106**:193–202 (2010).
4. A. Schirmer, M. A. Rude, X. Li, E. Popova, S. B. del Cardayre. Microbial biosynthesis of alkanes. *Science* **329**:559–562 (2010).
5. J. M. Perez, F. A. Arenas, G. A. Pradenas, J. M. Sandoval, C. C. Vasquez. *Escherichia coli* YqhD exhibits aldehyde reductase activity and protects from the harmful effect of lipid peroxidation-derived aldehydes. *J. Biol. Chem.* **283**:7346–7353 (2008).
6. Z. Fatma, K. Jawed, A. J. Mattam, S. S. Yazdani. Identification of long chain specific aldehyde reductase and its use in enhanced fatty alcohol production in *E. coli*. *Metab. Eng.* **37**:35–45 (2016).
7. C. W. Bradshaw, H. Fu, G. J. Shen, C. H. Wong. A *Pseudomonas* sp. alcohol dehydrogenase with broad substrate specificity and unusual stereospecificity for organic synthesis. *J. Org. Chem.* **57**:1526–1532 (1992).
8. B. Machielsen, A. R. Uria, S. W. M. Kengen, J. van der Oost. Production and characterization of a thermostable alcohol dehydrogenase that belongs to the aldo-keto reductase superfamily. *Appl. Environ. Microbiol.* **72**:233–238 (2006).
9. P. Koutsompogeras, A. Kyriacou, I. Zabetakis. Characterizing NAD-dependent alcohol dehydrogenase enzymes of *Methylobacterium extorquens* and strawberry (*Fragaria* × *ananassa* cv. Elsanta). *J. Agric. Food. Chem.* **54**:235–242 (2006).
10. Y. C. Park, K. Y. San, G. N. Bennett. Characterization of alcohol dehydrogenase 1 and 3 from *Neurospora crassa* FGSC2489. *Appl. Microbiol. Biotechnol.* **76**:349–356 (2007).
11. O. de Smidt, J. C. du Preez, J. Albertyn. The alcohol dehydrogenases of *Saccharomyces cerevisiae*: a comprehensive review. *FEMS Yeast. Res.* **8**:967–978 (2008).
12. Y. X. Cao, W. H. Xiao, J. L. Zhang, Z. X. Xie, M. Z. Ding, Y. J. Yuan. Heterologous biosynthesis and manipulation of alkanes in *Escherichia coli*. *Metab. Eng.* **38**:19–28 (2016).
13. T. P. Howard, S. Middelhaufe, K. Moore, C. Edner, D. M. Kolak, G. N. Taylor, D. A. Parker, R. Lee, N. Smirnoff, S. J. Aves, J. Love. Synthesis of customized petroleum-replica fuel molecules by targeted modification of free fatty acid pools in *Escherichia coli*. *Proc. Natl. Acad. Sci. U.S.A.* **110**:7636–7641 (2013).

14. D. M. Warui, N. Li, H. Nørgaard, C. Krebs, J. M. J. Bollinger, S. J. Booker. Detection of formate, rather than carbon monoxide, as the stoichiometric coproduct in conversion of fatty aldehydes to alkanes by a cyanobacterial aldehyde decarbonylase. *J. Am. Chem. Soc.* **133**:3316–3319 (2011).
15. J. T. Whitteck, R. M. Cicchillo, W. van der Donk. Hydroperoxylation by hydroxyethylphosphonate dioxygenase. *J. Am. Chem. Soc.* **131**:16225–16232 (2009).
16. R. M. Cicchillo, H. Zhang, J. A. V. Blodgett, J. T. Whitteck, G. Li, S. K. Nair, W. van der Donk, W. W. Metcalf. An unusual carbon–carbon bond cleavage reaction during phosphinothricin biosynthesis. *Nature* **459**:871–874 (2009).

SUPPLEMENTARY INFORMATION

Table S2.1 Nucleotide sequence of *PsADH*, *NpAD*, *Fd*, and *FNR* (For *Fd* and *FNR* genes, the codon is optimized for *E. coli* expression, showing as an underlined sequence)

>PsADH

ATGAACATGAAGATCAAAACCACGATGAAAGCGGCAGTTGTGAAATCGTTCGGTGAGCCT
TTGGTGATTGAAGAAGTACCGGTGCCTTCGGTCGGGCCGGGTCAGGTTTTGGTAAAAATT
GCCGCCACCGGGGTTTGCCATACCGATTTGCACGCTGCTGAAGGTGACTGGCCGATCAAA
CCTAATCCCCCCTTTATTCCCGGCCATGAAGGTGTTGGTCAGGTTGTGGCGCTGGGCGAA
GGTGTGAAACATCTCAAACTTGGCGATCGCGTGGGTGTGCCCTGGCTCTACTCGGCCTGT
GGTCATTGCGAATATTGTCTCGATAGCTGGGAAACGCTGTGTCTGTCGCAGCAGAATGCC
GGTTATTCAGTCAATGGTAGCTTTGCAGAGTATTGCCTGGCGGATGCTAACTACGTCGGT
ATCCTGCCGGATAATATTGAGTATCATGAGATCGCACCGATTTTGTGTGCCGGTGTCACG
GTGTACAAAGGGCTGAAGATGACCGATACCAAGCCAGGTGACTGGGTGGTGATTTCCGGT
ATCGGTGGTTTGGGACATATGGCTGTTCAGTACGCGGTAGCGATGGGGCTTAACGTGGCT
GCTGTTGATATTGATGACGAGAAGCTGGAGTTTGCTAAACGTCTGGGTGCCAGCGTGGTG
GCTAACGCGAAAAATGTCGATCCGGCGAAATTCTTCCACGAAAGCTTCGGCGGCGCGCAC
GGTGTGCTGGTGACAGCGGTTTCACCGAAAGCCTTTGAGCAAGCGTTGGGAACCATGCGT
CGTGGCGGTACGATGGTGCTGAATGGCCTGCCGCCGGGCAAATTTGACCTGTCGATTTTT
GACATGGTGTTGGACGGTATTACGGTGCGCGGTTCAATTGTCGGCACCCGTAAGGATTTG
CAGGAGGCGCTCGACTTCGCTGGTCGTCACAAAGTGAAAGCCAATGTAGCGGTGGAGCCG
TTGGTCAACATCAACGATATCTTTGCCCGCATGCATGCCGGTAAAATTGAAGGCCGTATT
GTTGTTGATATGTCGCTGTAA

>NpAD

ATGCAGCAGCTTACAGACCAATCTAAAGAATTAGATTTCAAGAGCGAAACATACAAAGAT
GCTTATAGCCGGATTAATGCGATCGTGATTGAAGGGGAACAAGAAGCCCATGAAAATTAC
ATCACACTAGCCCAACTGCTGCCAGAATCTCATGATGAATTGATTCGCCTATCCAAGATG
GAAAGCCGCCATAAGAAAGGATTTGAAGCTTGTGGGCGCAATTTAGCTGTTACCCCAGAT
TTGCAATTTGCCAAAGAGTTTTTCTCCGGCCTACACCAAAATTTTCAAACAGCTGCCGCA
GAAGGGAAAGTGGTTACTTGTCTGTTGATTCAGTCTTTAATTATTGAATGTTTTGCGATC
GCAGCATATAACATTTACATCCCCGTTGCCGACGATTTCGCCCGTAAAATTACTGAAGGA
GTAGTTAAAGAAGAATACAGCCACCTCAATTTTGGAGAAGTTTGGTTGAAAGAACACTTT
GCAGAATCCAAAGCTGAACTTGAACTTGCAAATCGCCAGAACCTACCCATCGTCTGGAAA
ATGCTCAACCAAGTAGAAGGTGATGCCCACACAATGGCAATGGAAAAAGATGCTTTGGTA
GAAGACTTCATGATTCAGTATGGTGAAGCATTGAGTAACATTGGTTTTTCGACTCGCGAT
ATTATGCGCTTGTCAGCCTACGGACTCATAGGTGCTTAA

>Fd

ATGGAACCGAAAACCTATACCGTGGAAATTGATCATCAGGGCAAAATCCATACCCTGCAG
GTGCCGGAAAACGAAACCATTCTGAGCGTTGCCGATGCCGCGGGCCTGGAACTGCCGAGC
AGCTGCAATGCGGGTGTTTGCACCACCTGTGCCGGCCAGATCAGCCAGGGTACCGTGGAT
CAGACCGATGGCATGGGTGTTAGCCCGGATCTGCAGAAACAGGGCTATGTGCTGCTGTGT
GTTGCCAAACCGCTGAGCGATCTGAAACTGGAAACCGAAAAAGAAGATATTGTGTATCAG
CTGCAGTTTGGTAAAGATAAATAA

>FNR

ATGGAATATAATCAGGGTGCCGTGGAAGGTGCCGCGAACATTGAACTGGGTAGCCGTATT
TTTGTCTATGAAGTGGTCGGTCTGCGTCAGGGTGAAGAAACCGATCAGACCAACTATCCG
ATCCGTAAAAGCGGCAGCGTGTTTATTCGTGTTCCGTATAACCGCATGAATCAGGAAATG
CGTCGCATTACCCGCCTGGGCGGTACCATTGTGAGCATCCAGCCGATTACCGCGCTGGAA
CCGGTTAACGGCAAAGCGAGCTTTGGTAATGCCACCAGCGTGGTTAGCGAACTGGCGAAA
AGCGGTGAAACCGCCAACAGCGAAGGCAATGGTAAAGCCACCCCGGTGAATGCGCATAGC
GCCGAAGAACAGAACAAAGATAAGAAAGGCAATACCATGACCCAGGCGAAAGCGAAGAAA
GATCATGGCGATGTGCCGGTTAACACCTATCGTCCGAATGCGCCGTTTATCGGCAAAGTG
ATTAGCAACGAACCGCTGGTTAAAGAAGGCGGTATTGGTATCGTGCAGCATCTGAAATTT
GATCTGAGCGGCGGTGATCTGAAATATATCGAAGGCCAGAGCATTGGTATTATCCCGCCG
GGCCTGGATAAAAATGGTAAACCGGAAAAACTGCGTCTGTATAGCATTGCGAGCACCCGT
CATGGCGATGATGTTGATGATAAAACCGTGAGCCTGTGCGTTCGTCAGCTGGAATATAAA
CATCCGGAAACCGGCGAAACCGTGTATGGTGTTTGCAGCACCCATCTGTGTTTTCTGAAA
CCGGGTGAAGAAGTGAAAATCACCGGCCCGGTTGGTAAAGAAATGCTGCTGCCGAACGAT
CCGGATGCGAATGTGATCATGATGGCAACCGGTACCGGTATTGCCCCGATGCGTGCCTAT
CTGTGGCGCCAGTTTAAAGATGCGGAACGCGCGGCCAACCCGGAATATCAGTTTAAAGGC
TTTAGCTGGCTGATTTTTGGTGTTCCGACCACCCCGAATCTGCTGTATAAAGAAGAACTG
GAAGAAATCCAGCAGAAATATCCGGAAAACTTTCGTCTGACCGCGGCCATTAGCCGCGAA
CAGAAAAATCCGCAGGGCGGTCGTATGTATATCCAGGATCGCGTGGCGGAACATGCCGAT
GAACTGTGGCAGCTGATCAAAAACGAAAAAACCCATACCTATATTTGTGGCCTGCGCGGT
ATGGAAGAAGGCATTGATGCCGCACTGACCGCGGCGGCGGCAAAAGAAGGTGTTACCTGG
TCGGATTATCAAAAACAACTGAAAAAGGCTGGTCGTTGGCATGTGGAAACCTATTAA

Table S2.2 Primers used in this chapter

Primers	Sequence
T7-F	5′-TAATACGACTCACTATAGGG-3′
T7-R	5′-TAGTTATTGCTCAGCGGTGG-3′
Adh-AS SalF	5′-GGGGTCGACATGAACATGAAGATCAAAACCACGATGAAAGCG-3′
Adh-AS NotR	5′-AAAGCGGCCGCTTACAGCGACATATCAACAACAATACGGCCTTC-3′
NpAD NdeF	5′-GGGCATATGATGCAGCAGCTTACAGACCAATCTAAA-3′
NpAD XhoIR	5′-GGGCTCGAGTTAAGCACCTATGAGTCCGTAGGCTGA-3′

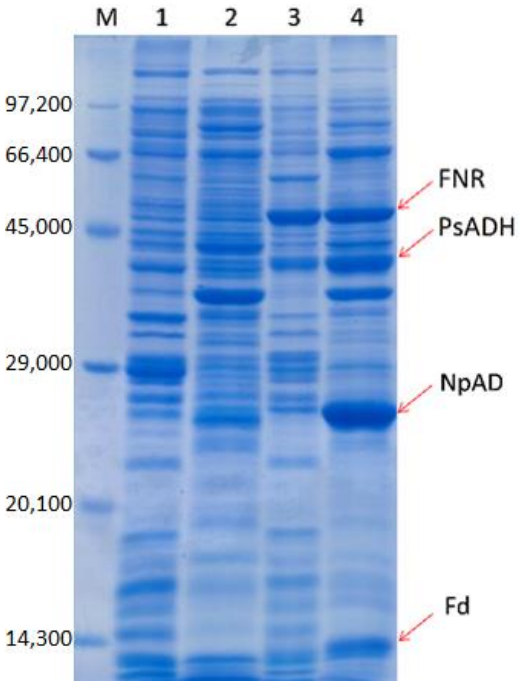

Figure S2.1 SDS-PAGE of protein fractions from transformed *E. coli* strains.

M, standard molecular weight.

1, insoluble protein fraction of *E. coli* Rosetta 2 (DE3)/pRSF/pCDF.

2, soluble protein fraction of *E. coli* Rosetta 2 (DE3)/pRSF/pCDF.

3, insoluble protein fraction of *E. coli* Rosetta 2 (DE3)/pRSF-*PsADH-NpAD*/pCDF-*Fd-FNR*.

4, soluble protein fraction of *E. coli* Rosetta 2 (DE3)/pRSF-*PsADH-NpAD*/pCDF-*Fd-FNR*.

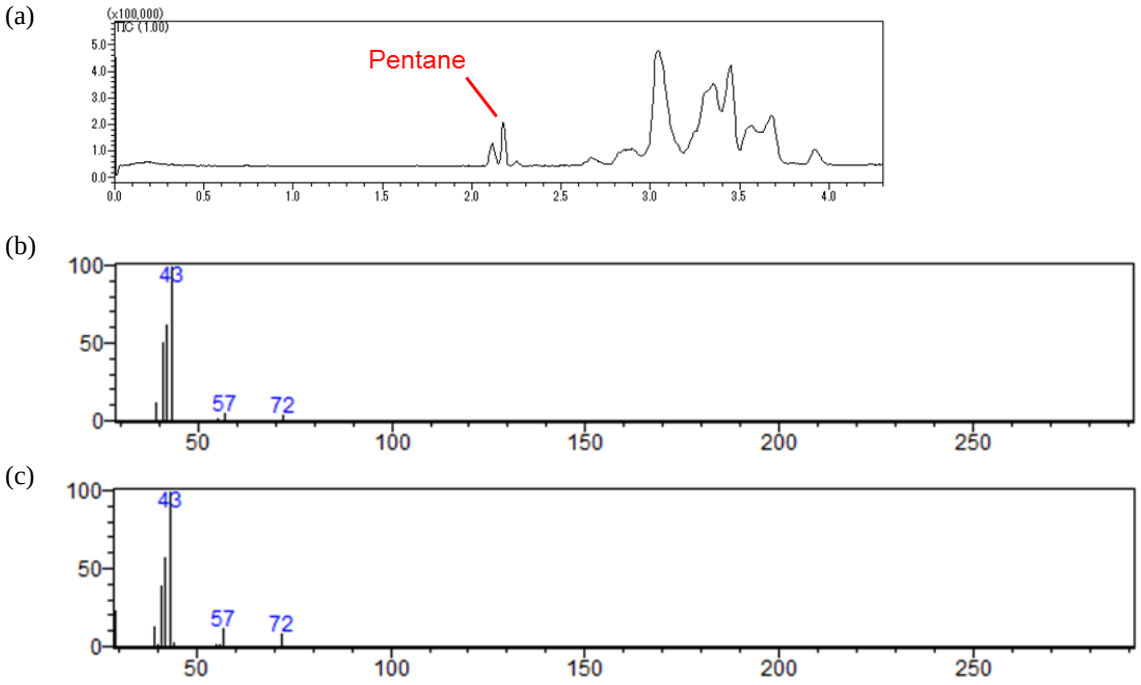

Figure S2.2 (a) GC-MS total ion chromatogram and (b) mass spectrum of pentane produced by *E. coli* expressing *PsADH-NpAD-Fd-FNR* from 1-hexanol. (c) Mass spectrum of pentane as similarity search result.

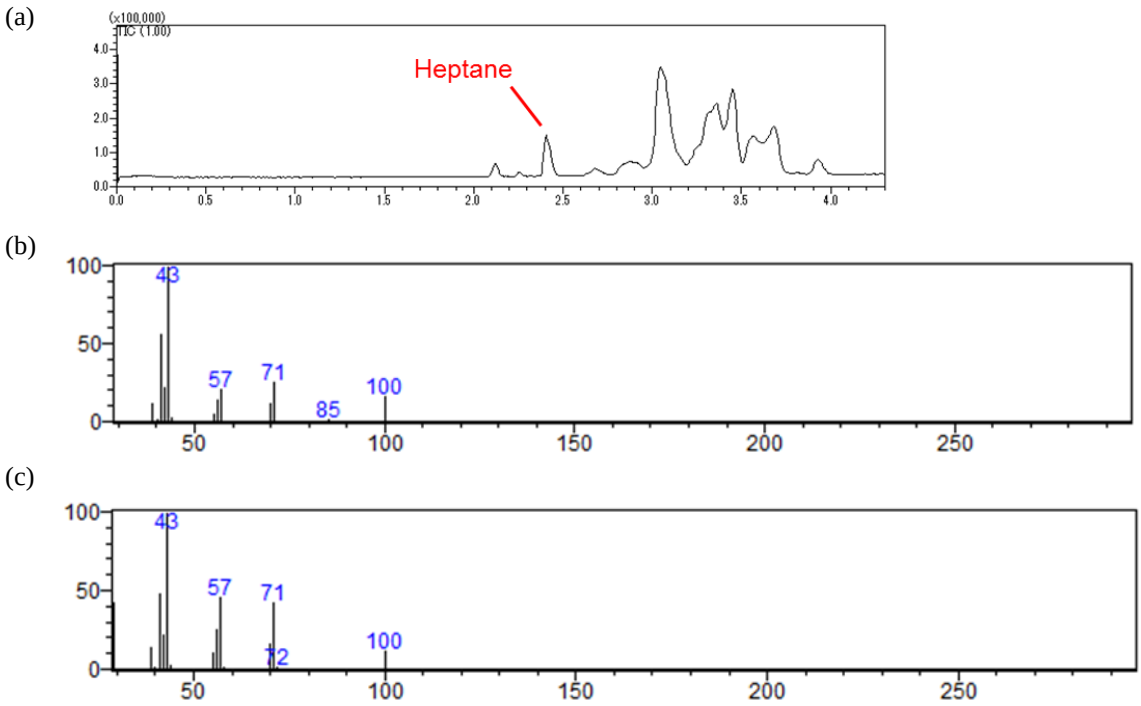

Figure S2.3 (a) GC-MS total ion chromatogram and (b) mass spectrum of heptane produced by *E. coli* expressing *PsADH-NpAD-Fd-FNR* from 1-octanol. (c) Mass spectrum of heptane as similarity search result.

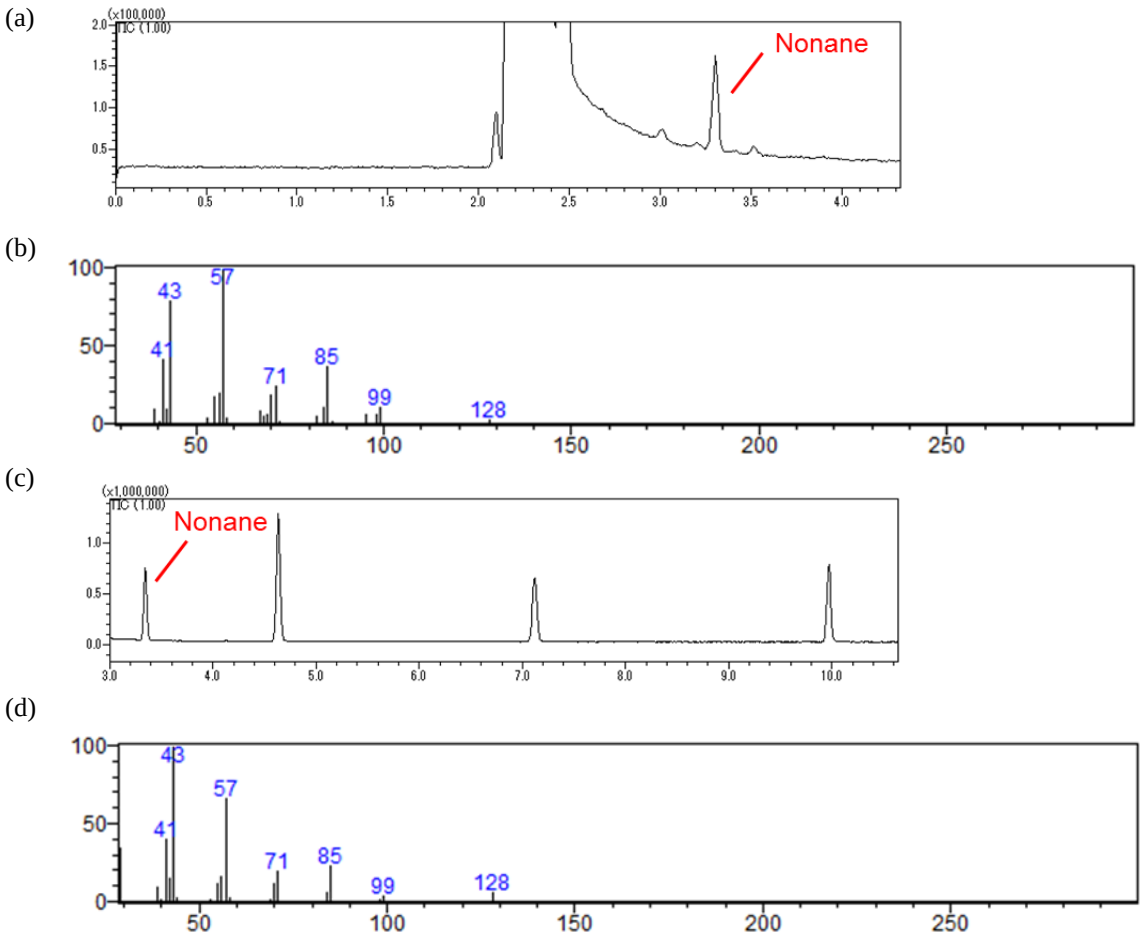

Figure S2.4 (a) GC-MS total ion chromatogram and (b) mass spectrum of nonane produced by *E. coli* expressing *PsADH-NpAD-Fd-FNR* from 1-decanol. (c) GC-MS total ion chromatogram and (d) mass spectrum of nonane standard compound.

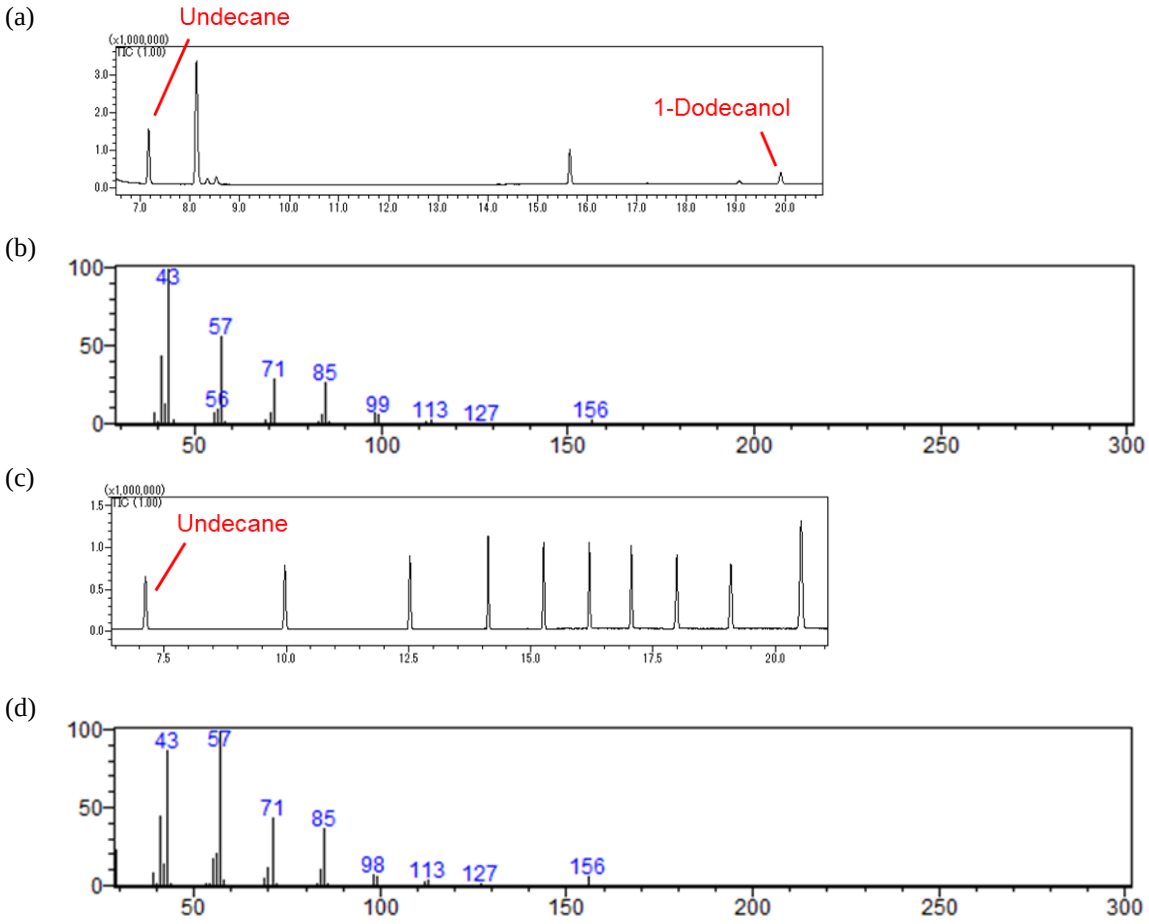

Figure S2.5 (a) GC-MS total ion chromatogram and (b) mass spectrum of undecane produced by *E. coli* expressing *PsADH-NpAD-Fd-FNR* from 1-dodecanol. (c) GC-MS total ion chromatogram and (d) mass spectrum of undecane standard compound.

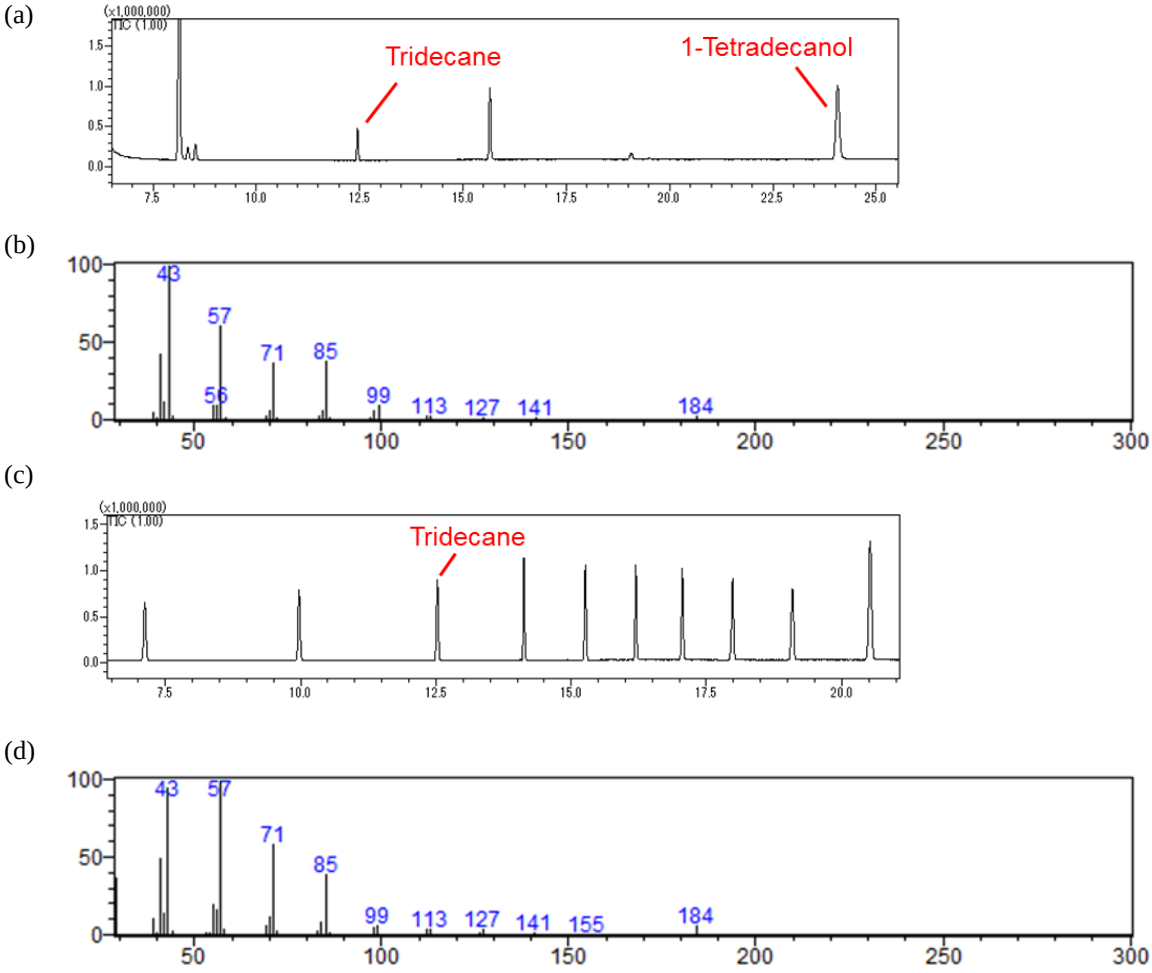

Figure S2.6 (a) GC-MS total ion chromatogram and (b) mass spectrum of tridecane produced by *E. coli* expressing *PsADH-NpAD-Fd-FNR* from 1-tetradecanol. (c) GC-MS total ion chromatogram and (d) mass spectrum of tridecane standard compound.

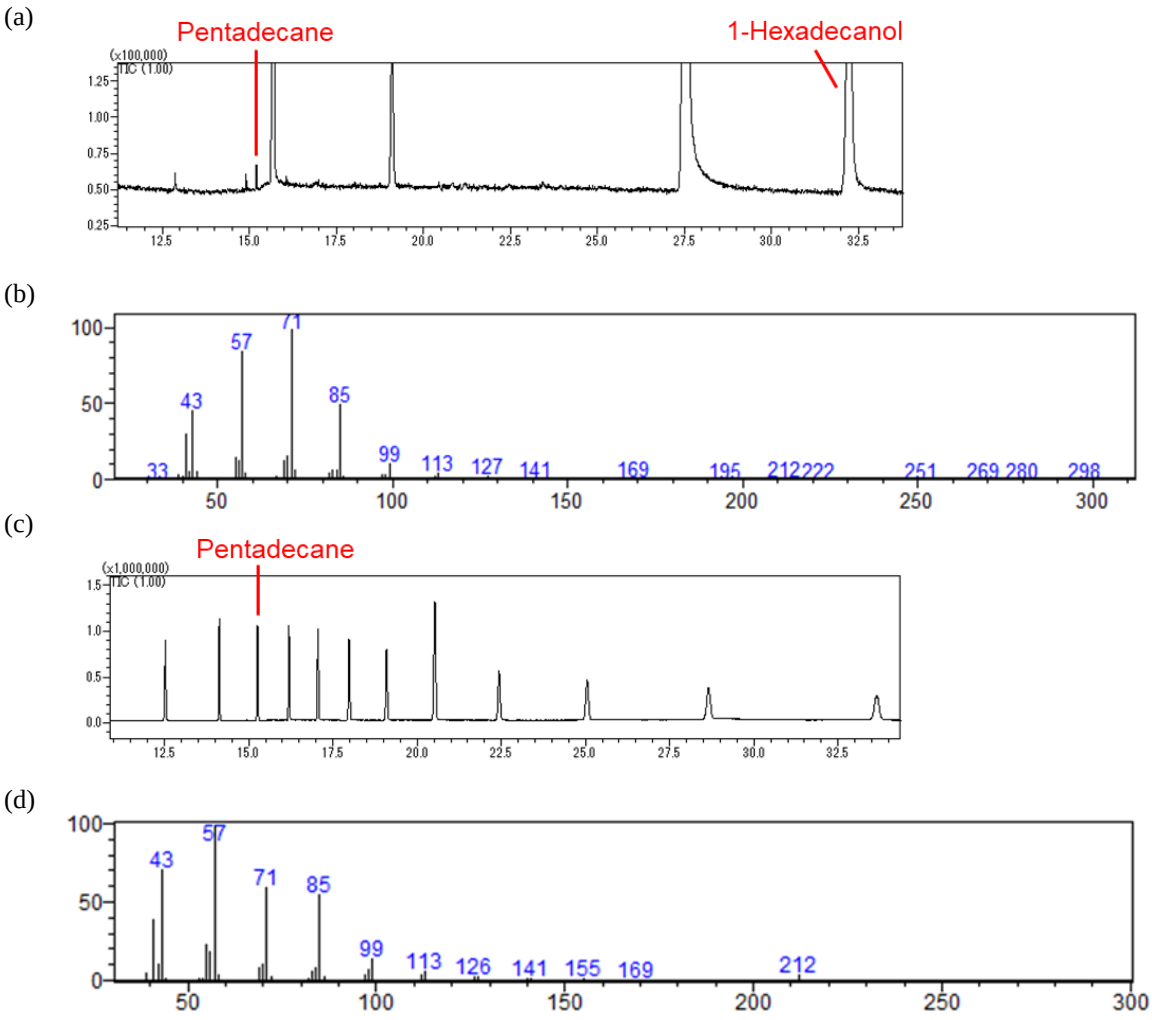

Figure S2.7 (a) GC-MS total ion chromatogram and (b) mass spectrum of pentadecane produced by *E. coli* expressing *PsADH-NpAD-Fd-FNR* from 1-hexadecanol. (c) GC-MS total ion chromatogram and (d) mass spectrum of pentadecane standard compound.

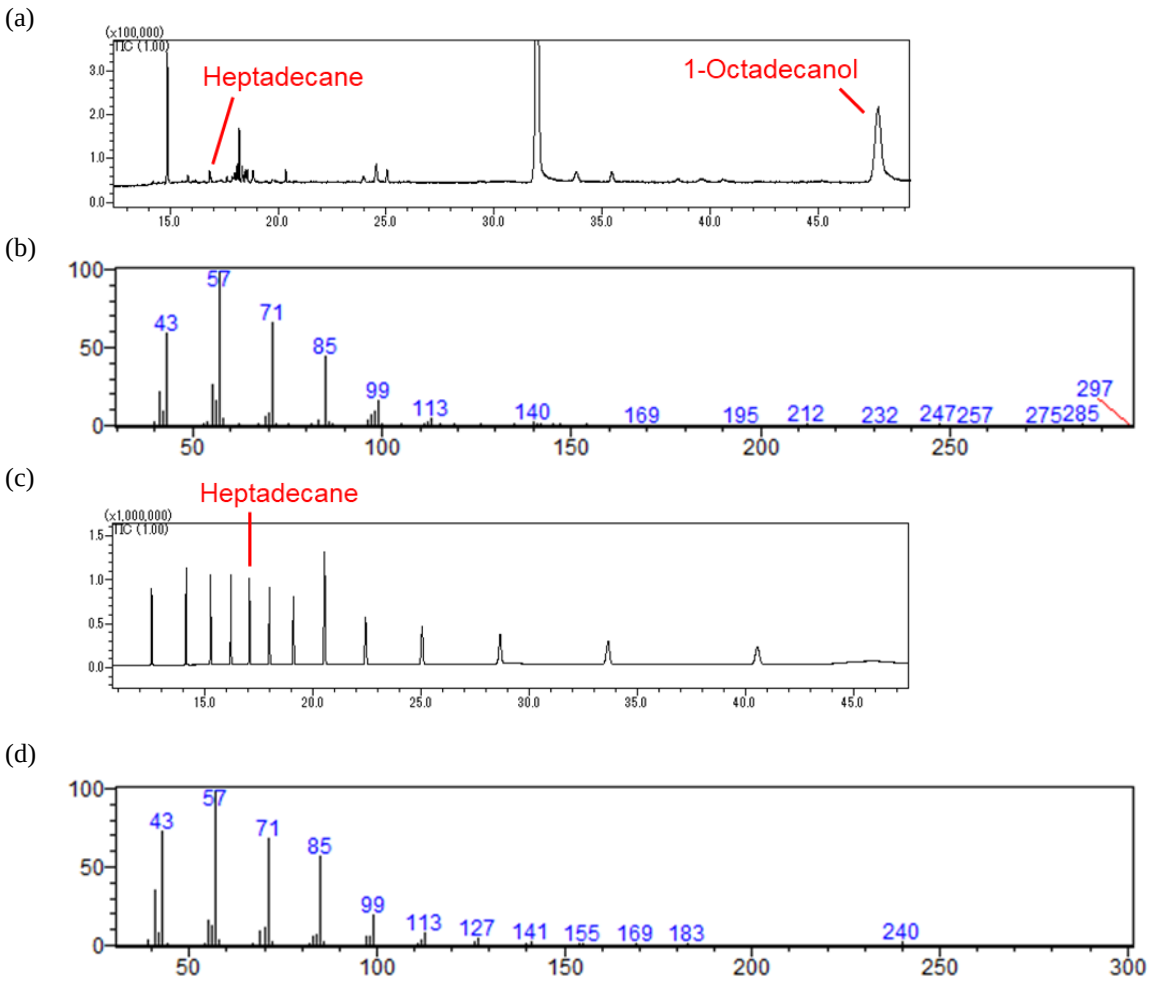

Figure S2.8 (a) GC-MS total ion chromatogram and (b) mass spectrum of heptadecane produced by *E. coli* expressing *PsADH-NpAD-Fd-FNR* from 1-octadecanol. (c) GC-MS total ion chromatogram and (d) mass spectrum of heptadecane standard compound.

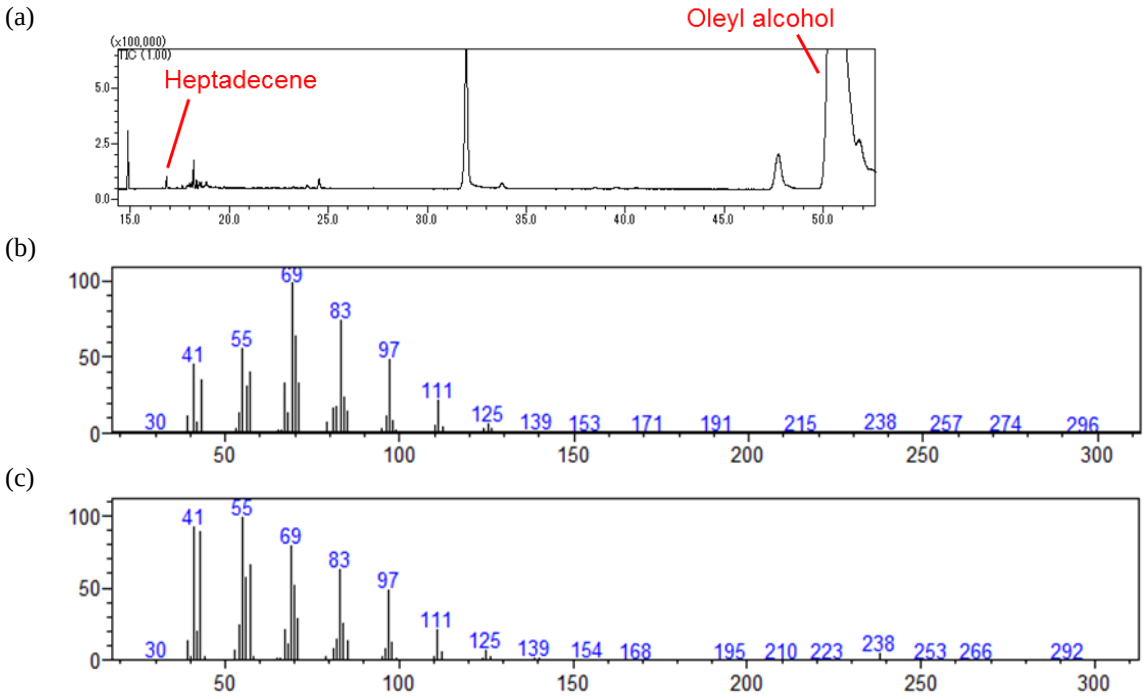

Figure S2.9 (a) GC-MS total ion chromatogram and (b) mass spectrum of heptadecene produced by *E. coli* expressing *PsADH-NpAD-Fd-FNR* from oleyl alcohol. (c) Mass spectrum of heptadecene as similarity search result.

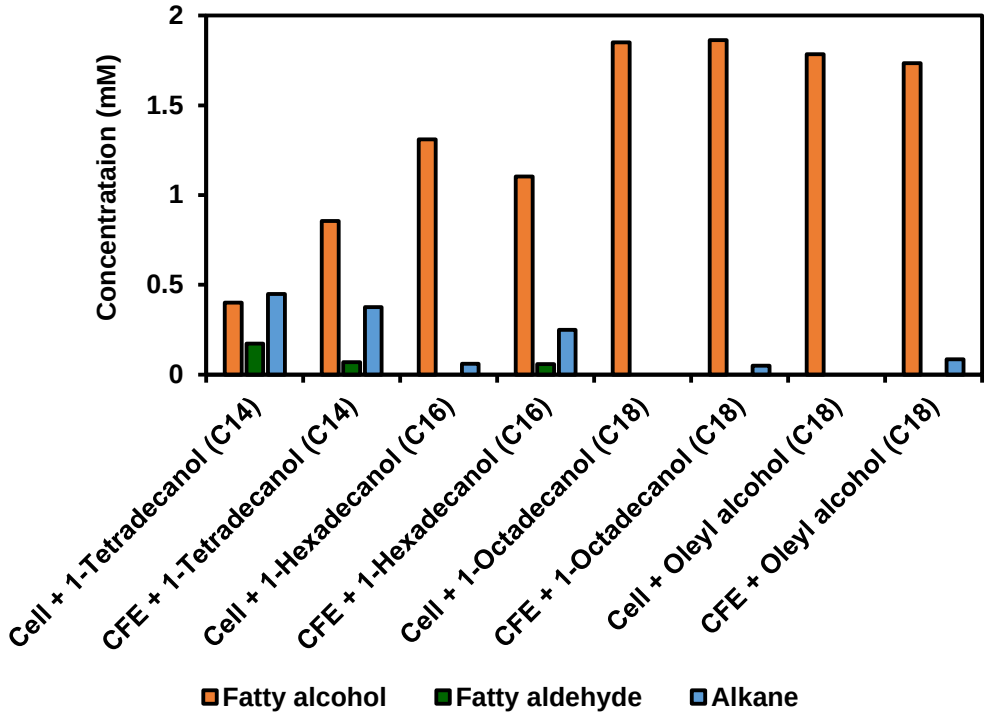

Figure S2.10 Substrate specificity of the cell-free extracts (CFE) obtained from *E. coli* cells expressing *PsADH-NpAD-Fd-FNR*.

CHAPTER 3

Application of fatty alcohol dehydrogenase PsADH to fermentative production of alkanes

INTRODUCTION

In the past few decades, biofuels such as bioethanol and biodiesel have been developed as substitution to fossil fuels. However, the performance of these biofuels were not as good as traditional fossil fuels because of their low energy density and relatively high hydrophilicity (1). On the other hand, bio-based hydrocarbons, such as alkanes and alkenes, are designed to share similar chemical composition as fossil fuels and expected to be used as drop-in biofuels (2).

A promising way to produce bio-alkanes is to construct metabolic engineered microorganisms harboring alkane biosynthetic pathway. For example, it is reported that by the heterologous expression of cyanobacterial fatty acyl-ACP and aldehyde-deformylating oxygenase in *E. coli*, alkane can be produced from carbon source, via the intermediates in fatty acid metabolism (3). Numerous studies have also reported the biosynthesis of alkanes in other metabolic engineered microorganisms such as *Saccharomyces cerevisiae* by applying the pathway mentioned above (4, 5). To date, studies have focused on the manipulation of upstream fatty acid metabolism of host microorganisms in order to produce more fatty acids and fatty aldehydes for alkane production (6, 7), however, the resulting alkane titers were lower than those current-used biofuels (8).

One of the bottlenecks in the biosynthesis of alkanes in engineered microorganisms such as *E. coli* was caused by the endogenous aldehyde reductases which are active in converting the intermediate fatty aldehydes to fatty alcohols (9, 10). Studies have shown that the deletion of aldehyde reductase genes in *E. coli* leads to a higher production of alkanes (11, 12), indicating the importance of eliminating the amount of intracellular fatty alcohols. However, it is hard to remove all aldehyde reductases, and the deletion of these genes will affect the cell growth. In chapter 1, the discovery of a fatty alcohol dehydrogenase PsADH was demonstrated, and the results revealed the potential of improving alkane production by applying this newly found enzyme to the alkane biosynthetic pathway. Furthermore, based on the result in chapter 2, the combination of PsADH with NpAD led to the direct production of alkanes from fatty alcohols, including alkanes with the same chain length as those reported to date (3).

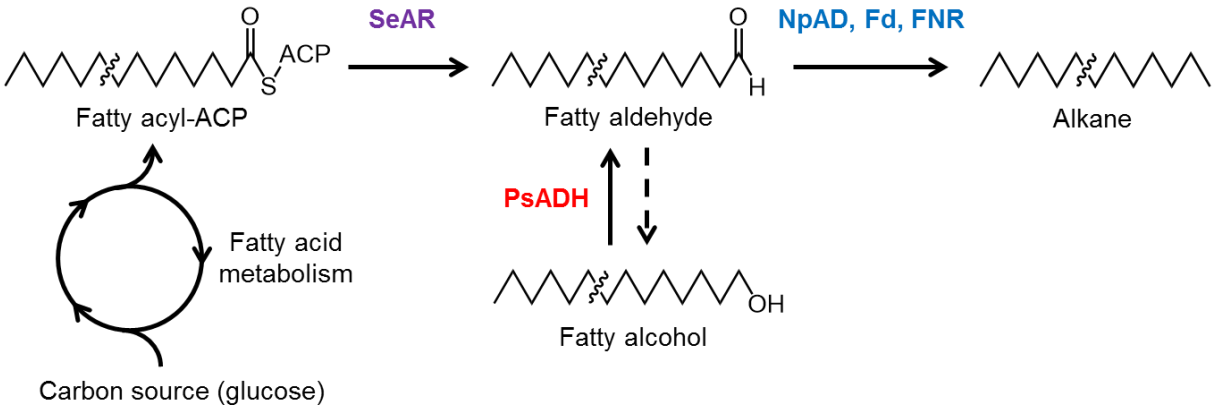

Scheme 3.1 Target reaction discussed in this chapter. PsADH, alcohol dehydrogenase. NpAD, aldehyde-deformylating oxygenase. Fd, ferredoxin. FNR, ferredoxin reductase. SeAR, acyl-ACP reductase.

Here in this chapter, the study focuses on the introduction of PsADH to alkane biosynthetic pathway. By coupling PsADH with SeAR, a fatty acyl-ACP reductase originated from *Synechococcus elongatus* PCC7942 as well as NpAD, the aldehyde-deformylating oxygenase used in previous chapter, the effect of alcohol dehydrogenation reaction contributed by PsADH could be evaluated (Scheme 3.1). During the fermentative alkane production, it is expected that PsADH will facilitate the reaction by regenerating the necessary fatty aldehyde from the accumulated fatty alcohol byproducts. Considering the lack of study concerning the utilization of fatty alcohols, this work will provide a new approach to produce alkanes efficiently.

MATERIALS AND METHODS

Chemicals, microbial strains, nucleotide sequences, primers, and plasmids

Chemicals were purchased from Fujifilm Wako Pure Chemical Corporation (Osaka, Japan). *E. coli* DH5α and *E. coli* Rosetta 2 (DE3) (Merck, Darmstadt, Germany) was used as host for heterologous gene expression. The nucleotide sequences of *SeAR* from *Synechococcus elongatus* PCC7942 (Table S3.1) and the primers (Table S3.2) used in this chapter are shown in the supplementary information. Other nucleotide sequences are shown in the supplementary information in previous chapters. The plasmid pRSFDuet-1 and pCDFDuet-1 (Merck) were used as the expression vectors.

Construction of alkane-producing *E. coli* transformants

The pRSFDuet-1 and pCDFDuet-1 vectors harboring the genes encoding alcohol dehydrogenase (*PsADH*, DDBJ accession number LC727629) from *Pantoea* sp. 7-4 as well as cyanobacterial aldehyde deformelating oxygenase (*NpAD*, NCBI accession number WP_012408400), ferredoxin (*Fd*, NCBI accession number WP_012408585), and ferredoxin $NADP^+$-reductase (*FNR*, NCBI accession number WP_012409282) from *Nostoc punctiforme* PCC73102 were mentioned in previous chapters, and were constructed as pRSF-*PsADH-NpAD* and pCDF-*Fd-FNR*. In this chapter, the vector pRSF-*PsADH-NpAD-SeAR* was constructed by inserting the gene encoding acyl-ACP reductase (*SeAR*, NCBI accession number WP_011242364) from *Synechococcus elongatus* PCC7942 to the vector pRSF-*PsADH-NpAD* using the following method. The *SeAR* gene and pRSF-*PsAdhP-NpAD* vector were amplified by PCR with the primer pairs of SeAR-SLiCE-F and SeAR-SLiCE-R, and pRSFSuet-Stag-Fw and pRSFDuet-Stag-rbs-Rv, respectively, showing in Table S3.2. The PCR was performed using PrimeSTAR MAX DNA polymerase (Takara Bio, Shiga, Japan) under the following reaction conditions: 94°C for 2 min and 35 cycles of 98°C for 10 s, 55°C for 5 s, and 72°C for 1.5 min. The amplified *SeAR* gene was inserted into the linear pRSF-*PsADH-NpAD* vector by Seemless Ligation Cloning Extract (SLiCE) method (13). The same method was used to construct the vector pRSF-*NpAD-SeAR*. The constructed vectors were transformed into *E. coli* Rosetta 2 (DE3), resulting in two *E. coli* transformants: the control strain *E. coli* Rosetta 2 (DE3)/pRSF-*NpAD-SeAR*/pCDF-*Fd-FNR*, and the ADH strain *E. coli* Rosetta 2 (DE3)/pRSF-*PsADH-NpAD-SeAR*/pCDF-*Fd-FNR*.

Alkane productivity assay

The *E. coli* transformants were cultivated in 10 mL LB medium containing chloramphenicol, kanamycin, and streptomycin at 37°C with shaking. For medium selection experiment, the medium was changed to 2×YT medium or modified M9 medium. The 2×YT medium consisted of 16 g/L tryptone,

10 g/L yeast extract, and 5 g/L NaCl. The modified M9 medium consisted of 12.8 g/L $Na_2HPO_4 \cdot 7H_2O$, 3 g/L KH_2PO_4, 0.5 g/L NaCl, 1 g/L NH_4Cl, 0.25 g/L $MgSO_4 \cdot 7H_2O$, 0.015 g/L $CaCl_2 \cdot 2H_2O$, 2 g/L yeast extract, and 0.2% (v/v) glycerol. When the optical density at 600 nm (OD_{600}) of the medium reached 0.8, the gene expression was induced with 0.5 mM IPTG and cultivated at 30°C with shaking. Protein expression was monitored by SDS-PAGE. After cultivated for 72 h, the medium was extracted with 1 mL toluene containing 1-pentadecanol as the internal standard and subjected to GC and GC-MS analysis.

GC and GC-MS analysis

The GC analysis was conducted using a Shimadzu GC-2010 Plus gas chromatograph (Shimadzu, Kyoto, Japan) equipped with a flame ionization detector and a Nukol capillary column (30 m × 0.25 mm × 0.25 μm; Supelco, Bellefonte, PA, USA). Helium at a flow rate of 1.12 ml/min was used as the carrier gas. Samples were injected with a split ratio of 50:1. The heating program of the column consisted of the following steps: the initial column temperature of 80°C was raised to 112°C at a rate of 5°C/min, then raised to 190°C at a rate of 40°C/min, and held at 190°C for 65 min. The GC-MS analysis was conducted using a Shimadzu GC-MS QP2010 (Shimadzu, Kyoto, Japan) with the same column and the same heating program described above. The mass spectrometer was operated in the electron impact mode at 70 eV, with an ion source temperature of 200°C.

Culture condition of fermentative production of alkane using jar fermenter

The constructed *E. coli* transformant, the ADH strain or the control strain, was inoculated in 30 mL 2×YT medium containing necessary antibiotics and cultivated overnight at 37°C with shaking. This 30 mL seed culture was then inoculated into 2.5 L fresh 2×YT medium containing 0.01% antiformer and necessary antibiotics in a jar fermenter with a total capacity of 5 L (ABLE Corporation, Tokyo, Japan). The jar fermenter was applied air pressure at 0.1 MPa and aerated at 3 L/min. The pH of the culture was controlled at 7.2 using 3 N NaOH. At first, the culture was incubated at 37°C and stirred at 300 rpm. Once the OD_{600} reached 0.7, gene expression was induced by adding IPTG at a concentration of 0.5 mM. After the addition of IPTG, the temperature was changed to 30°C and the stirring speed was changed to 200 rpm for 3 h. After incubated for 3 h, the stirring speed was changed back to 300 rpm. Glucose was added at a final concentration of 1% at the time point of 8, 24, and 48 h, and at a final concentration of 2% at the time point of 72 and 96 h. The culture medium was sampled at 0, 8, 24, 48, 72, 96, and 144 h. The sample was extracted with toluene and analyzed by GC and GC-MS.

RESULTS

Construction of alkane-producing *E. coli* strains

To evaluate the effect of PsADH on the alkane production, two *E. coli* transformants were first constructed, naming the control strain and the ADH strain. The control strain harbored *NpAD*, *SeAR*, *Fd*, and *FNR* genes, while the ADH strain harbored *PsADH*, *NpAD*, *SeAR*, *Fd*, and *FNR* genes. The control strain possessed the necessary genes that enabled it to produce alkanes from carbon source. The ADH strain possessed the gene of PsADH in addition to those heterologous genes in the control strain. The protein expression was monitored by SDS-PAGE, shown in Figure S3.1 in supplementary information.

Alkane productivity assay and analysis of products

The alkane productivity assay conducted in 10 mL LB medium revealed that the alkane-producing *E. coli*, the control strain and the ADH strain, produced various kinds of fatty alcohols and alkanes. GC-MS was conducted to identify the products generated from *E. coli*. As shown in Figure 3.1, the ADH strain was found to produce hydrocarbons including tridecane, pentadecane, and heptadecene. Note that heptadecene is an alkene but not alkane. However, for simplicity, the word alkane is used in this study when mentioning all kinds of hydrocarbon, including heptadecene. Also, the alcohols including 1-tetradecanol, 1-hexadecanol, and oleyl alcohol were also detected. These alcohols were known to be derived from aldehyde intermediates by the reaction catalyzed by endogenous aldehyde reductases.

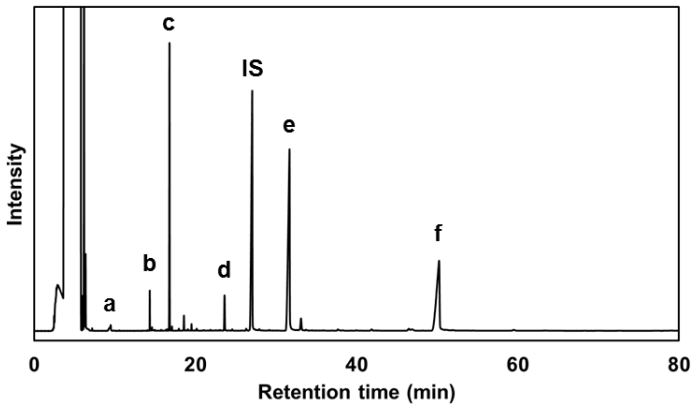

Figure 3.1 GC chromatogram of the products generated by *E. coli* expressing *PsADH-NpAD-SeAR-Fd-FNR* (ADH strain). IS indicates the internal standard (1-Pentadecanol). (a) Tridecane. (b) Pantadecane. (c) Heptadecene. (d) 1-Tetradecanol. (e) 1-Hexadecanol. (f) Oleyl alcohol.

Medium selection for alkane fermentation

The medium used for alkane fermentation was evaluated. The ADH strain was cultivated in three different kinds of medium (modified M9 medium, LB medium, and 2×YT medium) for 72 h, and their alkane and alcohol production was analyzed (Figure 3.2). Although the accumulation of alcohols was the highest (0.63 mM) when the cells were cultivated in 2×YT medium, the alkane production was also the highest among three kinds of medium. Considering the need of conducting alkane fermentation in a long period, the medium with higher nutrient concentration will be more suitable. As a result, 2×YT medium was selected for conducting further experiments in this study.

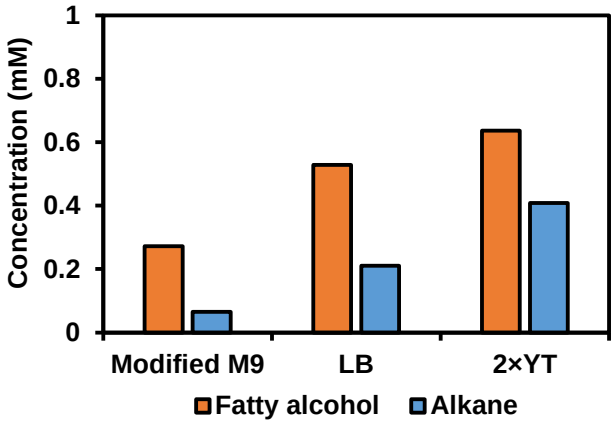

Figure 3.2 Fatty alcohol and alkane concentration in the 10 mL medium cultivating the ADH strain.

Fermentative production of alkane using jar fermenter

The fermentative production of alkanes was conducted in a jar fermenter containing 2.5 L medium. The cell growth, pH and the titer of products during the six-day cultivation time were monitored. The time course analysis revealed that the control strain produced the highest amount of total fatty alcohols at 144 h, with an amount of 4.37 mM (Figure 3.3a). On the other hand, the ADH strain produced the highest amount of total fatty alcohols at 96 h, with an amount of 2.13 mM (Figure 3.3b). The result suggested that the introduction of PsADH reduced approximately 51% of the intracellular fatty alcohols. The highest alkane titer in the control strain was 0.36 mM, while the highest alkane titer of ADH strain was 1.31 mM. The introduction of PsADH led to a three-fold increase of alkane production. The final OD_{600} of the control strain was approximately 40, which is higher than that of the ADH strain.

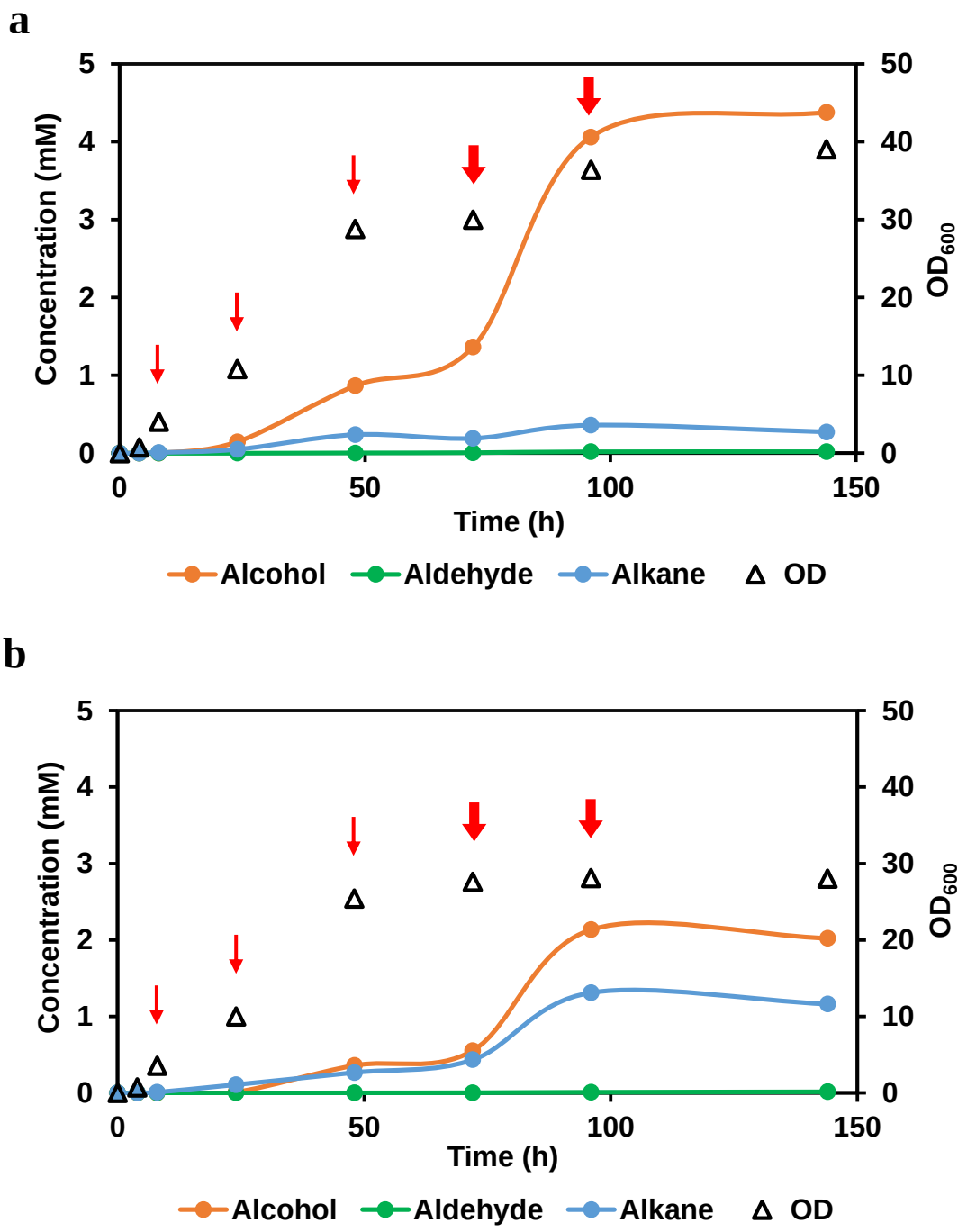

Figure 3.3 Time-course analysis of each product during the alkane fermentation process in jar fermenter. (a) Control strain. (b) ADH strain. OD_{600}, optical density at 600 nm. The red arrows indicate the time point of glucose feeding (1% glucose for 8, 24, and 48 h; 2% glucose for 72 and 96 h).

Product profile of alkane fermentation

The products generated by the control strain and the ADH strain were analyzed (Figure 3.4). The species of alcohols and alkanes produced in the jar fermenter were the same as those found in the test tube scale in the previous section (Figure 3.1). During the first 24 h, the alkane titer of the ADH strain was approximately the same as that of the control strain, however, the ADH strain produced much more alkanes afterwards (Figure 3.4a). The main components of alkanes were heptadecene and pentadecane for both strains, however, the total alkane titer in the ADH strain was much higher than that in the control strain. Tridecane was also detected, with approximately the same amount in both strains. For alcohols, the ADH strain produced a significantly lower amount of oleyl alcohol than the control strain (0.63 mM and 1.82 mM respectively, Figure 3.4b), which was expected to be contributed by the introduction of PsADH. 1-Hexadecanol was also one of the main byproducts found in both strains. Again, the ADH strain produced less amount of 1-hexadecanol than the control strain (1.32 mM and 2.19 mM respectively, Figure 3.4b).

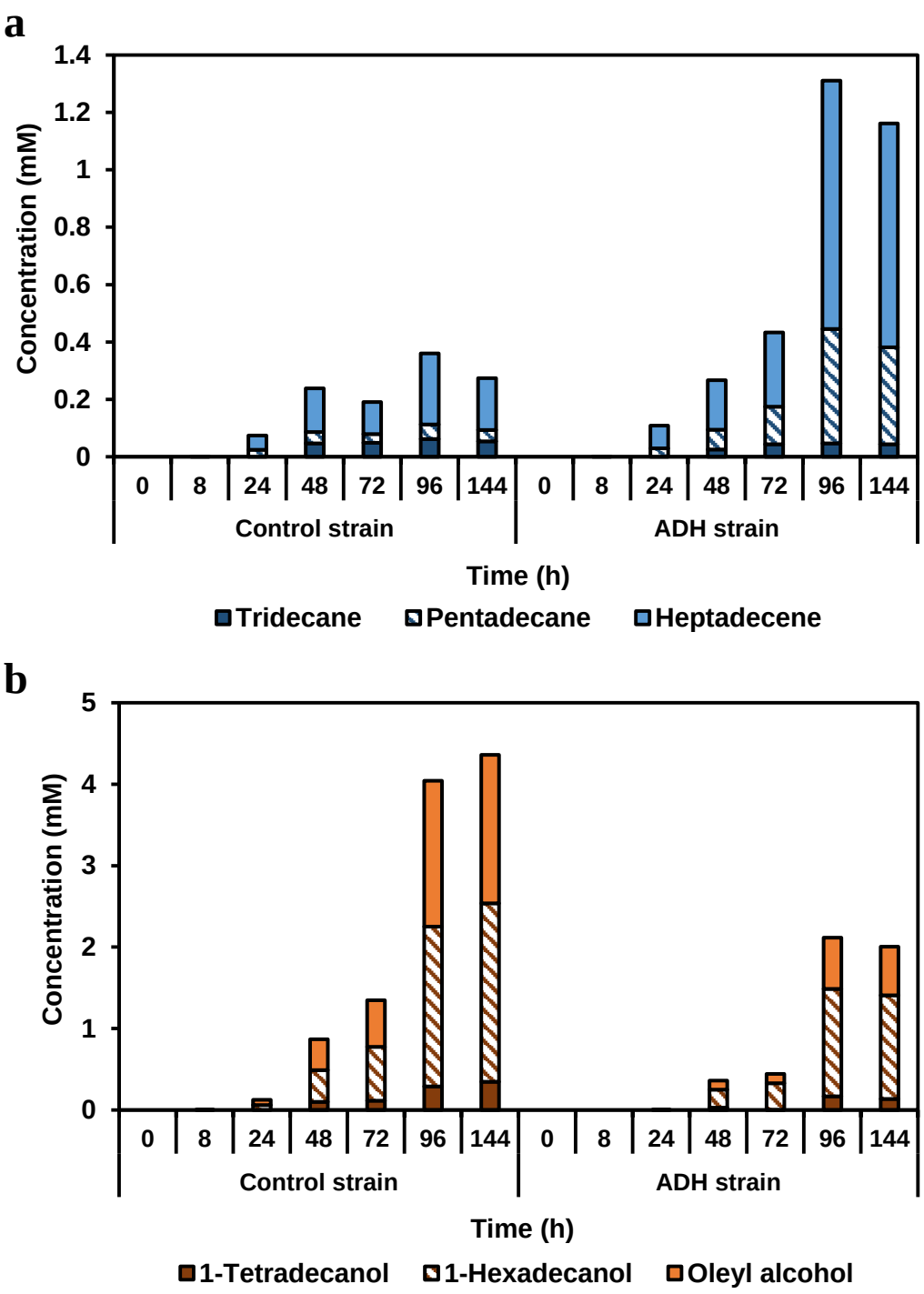

Figure 3.4 Time-course qualification and quantification of products generated during the alkane fermentation process in jar fermenter. (a) Alkanes. (b) Fatty alcohols.

DISCUSSION

The biosynthesis of alkanes in *E. coli* is strongly limited by the endogenous aldehyde reductases which are active in reducing fatty aldehydes into fatty alcohols. In this study, a new approach was demonstrated to solve such problem. An alcohol dehydrogenase with activity toward medium-chain fatty alcohols was discovered and characterized during the previous screening of soil-isolated microorganisms. In this chapter, this newly found enzyme PsADH was applied to the alkane biosynthetic pathway composed of a cyanobacterial acyl-ACP reductase SeAR and an aldehyde-deformylating oxygenase NpAD.

According to Figure 3.3, the strain containing PsADH produced significantly more alkanes and less alcohols comparing to the strain without PsADH during alkane fermentation process. Detailed analysis of product profile revealed that three kinds of alkanes (tridecane, pentadecane, and heptadecene) and their corresponding fatty alcohols (1-tetradecanol, 1-hexadecanol, oleyl alcohol, resepectively) were detected in the medium (Figure 3.4). Note that in chapter 2, it was found that the *E. coli* expressing *PsADH-NpAD-Fd-FNR* genes was not able to produce heptadecene from oleyl alcohol in the reaction using resting cells as the source of enzymes. The result in this study as well as other previous studies (3), however, suggested that the expression of cyanobacterial acyl-ACP reductase and aldehyde-deformylating oxygenase could lead to the production of heptadecene from carbon source such as glucose. Therefore, it is assumed that the key to produce long-chain alkanes is to generate fatty aldehydes intracellularly as the substrate for aldehyde-deformylating oxygenase. As discussed in the previous chapter, since long-chain alcohols such as oleyl alcohol has very low solubility in water, only a trace amount of substrates could enter the cell and be converted to aldehydes by PsADH in the reaction using resting cells. The result in Figure 3.4 also suggested that the chain length of final alkane products is limited to medium-to-long chain (C13–C17 alkanes / alkenes) which is derived from the chain length of fatty acyl-ACP generated. Although PsADH has a broad substrate spectrum that it could oxidize alcohols ranging from C6–C18 into aldehydes, gene modification toward upstream fatty acid metabolism remains necessary when producing alkanes with chain length shorter than C13.

The fermentation process constructed in this study successfully demonstrated the effect of adding PsADH to alkane production, however, more efforts remained in need to produce alkane at a higher titer. For example, the time course analysis in Figure 3.3 raised an issue that the cells in jar fermenter may not maintain a good condition for long, showing by the steady level of OD_{600} and alkane production after 96 h. Glucose at a final concentration of 2% was added every 24 hours in the jar fermenter to maintain cell growth, however, more nutrients such as the components of the organic material (tryptone

and yeast extract) may also be required to facilitate the growth as well as the gene expression. Additional antibiotics are also considered to be added after 24 hours to prevent the depletion of antibiotics.

Besides the growth condition, the balance between each component involved in the alkane-producing reaction plays an important role in perfecting the efficiency. For example, a cofactor regeneration system Fd and FNR was incorporated to regenerate NADPH which is required by the decarbonylation reaction catalyzed by NpAD (14). On the other hand, the cellular concentration of NAD^+/NADH may lose balance throughout the fermentation progress since PsADH requires NAD^+ as cofactor. Furthermore, a one-carbon moiety compound, determined as formic acid which is described in chapter 2 and previous studies (15), is generated per turnover when NpAD catalyze the decarbonlyation of aldehydes. The accumulation of the byproduct formic acid may decrease the pH and the enzymes may lose their activity. To prevent this, the culture broth was monitored and control at a neutral environment (pH 7.2) throughout the fermentation process by adding NaOH. A previous study has also reported that the introduction of a formate dehydrogenase could help maintain the cellular pH and increase alkane yield in the alkane-producing *E. coli* by converting formic acid to carbon dioxide (16). The synergy of formate dehydrogenase and PsADH, including the balance of the cofactors involved in the reactions catalyzed by these enzymes, required to be studied in the future research.

Overall, the results in this chapter demonstrated the feasibility of PsADH when applying it to the alkane biosynthetic pathway. By re-oxidizing a wide range of fatty alcohols to fatty aldehydes, PsADH provides the aldehyde-deformylating oxygenase with a more sufficient amount of substrates, leading to a higher alkane titer. The work in this study will provide a new solution to the byproduct issue in the microbial production of alkanes.

SUMMARY

Alkanes produced from renewable biomass are expected to be a superior alternative to the currently used biofuels because they are chemically similar to petroleum and can serve as drop-in fuels. Recent studies have reported the biosynthesis of alkanes by heterologous expression of cyanobacterial fatty acyl-ACP reductase and aldehyde-deformylating oxygenase in *Escherichia coli*. Nevertheless, the alkane titer in *E. coli* was low due to the endogenous aldehyde reductases which reduce the important intermediate, fatty aldehydes, into fatty alcohols. Here, the introduction of a newly-discovered alcohol dehydrogenase, PsADH, was demonstrated to re-oxidize the accumulated alcohol byproducts to fatty aldehydes for alkane production. The data in this study suggested that by co-expressing PsADH with the enzymes involved in alkane biosynthesis, the alkane titers increased 3.6 fold during the fermentation. Further analysis of the time course and the product profile of the alkane-fermenting process revealed the detailed variation of each product and demonstrated the effect of PsADH in facilitating alkane production.

REFERENCES

1. Y. H. Yoo, I. J. Park, J. G. Kim, D. H. Kwak, W. S. Ji. Corrosion characteristics of aluminum alloy in bio-ethanol blended gasoline fuel: Part 1. The corrosion properties of aluminum alloy in high temperature fuels. *Fuel* **90**:1208–1214 (2011).
2. R. M. Lennen, D. J. Braden, R. M. West, J. A. Dumesic, B. F. Pfleger. A process for microbial hydrocarbon synthesis: overproduction of fatty acids in *Escherichia coli* and catalytic conversion to alkanes. *Biotechnol. Bioeng.* **106**:193–202 (2010).
3. A. Schirmer, M. A. Rude, X. Li, E. Popova, S. B. del Cardayre. Microbial biosynthesis of alkanes. *Science* **329**:559–562 (2010).
4. N. A. Buijs, Y. J. Zhou, V. Siewers, J. Nielsen. Long-chain alkane production by the yeast *Saccharomyces cerevisiae*. *Biotechnol. Bioeng.* **112**:1275–1279 (2015).
5. Y. J. Zhou, N. A. Buijs, Z. Zhu, J. Qin, V. Siewers, J. Nielsen. Production of fatty acid-derived oleochemicals and biofuels by synthetic yeast cell factories. *Nat. Commun.* **7**:11709 (2016).
6. Y. J. Choi, S. Y. Lee. Microbial production of short-chain alkanes. *Nature* **502**:571–574 (2013).
7. Y. X. Cao, W. H. Xiao, J. L. Zhang, Z. X. Xie, M. Z. Ding, Y. J. Yuan. Heterologous biosynthesis and manipulation of alkanes in *Escherichia coli*. *Metab. Eng.* **38**:19–28 (2016).
8. Y. Xu, J. Li, M. Zhang, D. Wang. Modified simultaneous saccharification and fermentation to enhance bioethanol titers and yields. *Fuel* **215**:647–654 (2018).
9. J. M. Perez, F. A. Arenas, G. A. Pradenas, J. M. Sandoval, C. C. Vasquez. *Escherichia coli* YqhD exhibits aldehyde reductase activity and protects from the harmful effect of lipid peroxidation-derived aldehydes. *J. Biol. Chem.* **283**:7346–7353 (2008).
10. Z. Fatma, K. Jawed, A. J. Mattam, S. S. Yazdani. Identification of long chain specific aldehyde reductase and its use in enhanced fatty alcohol production in *E. coli*. *Metab. Eng.* **37**:35–45 (2016).
11. X. Song, H. Yu, K. Zhu. Improving alkane synthesis in *Escherichia coli* via metabolic engineering. *Appl. Microbiol. Biotechnol.* **100**:757–767 (2016).
12. G. M. Rodriguez, S. Atsumi. Toward aldehyde and alkane production by removing aldehyde reductase activity in *Escherichia coli*. *Metab. Eng.* **25**:227–237 (2014).
13. K. Motohashi. A simple and efficient seamless DNA cloning method using SLiCE from *Escherichia coli* laboratory strains and its application to SLiP site-directed mutagenesis. *BMC Biotechnol.* **15**:47 (2015).
14. L. J. Rajakovich, H. Nørgaard, D. M. Warui, W. C. Chang, N. Li, S. J. Booker, C. Krebs, J. M. J. Bollinger, M. E. Pandelia. Rapid reduction of the diferric-peroxyhemiacetal intermediate in

aldehyde-deformylating oxygenase by a cyanobacterial ferredoxin: evidence for a free-radical mechanism. *J. Am. Chem. Soc.* **137**:11695–11709 (2015).

15. D. M. Warui, N. Li, H. Nogaard, C. Krebs, J. M. J. Bollinger, S. J. Booker. Detection of formate, rather than carbon monoxide, as the stoichiometric coproduct in conversion of fatty aldehydes to alkanes by a cyanobacterial aldehyde decarbonylase. *J. Am. Chem. Soc.* **133**:3316–3319 (2011).
16. J. Jaroensuk, P. Intasian, C. Kiattisewee, P. Munkajohnpon, P. Chunthaboon, S. Buttranon, D. Trisrivirat, T. Wongnate, S. Maenpuen, R. Tinikul, P. Chaiyen. Addition of formate dehydrogenase increases the production of renewable alkane from an engineered metabolic pathway. *J. Biol. Chem.* **294**:11536-11548 (2019).

SUPPLEMENTARY INFORMATION

Table S3.1 Nucleotide sequence of *SeAR*

>SeAR

ATGTTCGGTCTTATCGGTCATCTCACCAGTTTGGAGCAGGCCCGCGACGTTTCTCGCAGGATGGGC
TACGACGAATACGCCGATCAAGGATTGGAGTTTTGGAGTAGCGCTCCTCCTCAAATCGTTGATGAA
ATCACAGTCACCAGTGCCACAGGCAAGGTGATTCACGGTCGCTACATCGAATCGTGTTTCTTGCCG
GAAATGCTGGCGGCGCGCCGCTTCAAAACAGCCACGCGCAAAGTTCTCAATGCCATGTCCCATGCC
CAAAAACACGGCATCGACATCTCGGCCTTGGGGGGCTTTACCTCGATTATTTTCGAGAATTTCGAT
TTGGCCAGTTTGCGGCAAGTGCGCGACACTACCTTGGAGTTTGAACGGTTCACCACCGGCAATACT
CACACGGCCTACGTAATCTGTAGACAGGTGGAAGCCGCTGCTAAAACGCTGGGCATCGACATTACC
CAAGCGACAGTAGCGGTTGTCGGCGCGACTGGCGATATCGGTAGCGCTGTCTGCCGCTGGCTCGAC
CTCAAACTGGGTGTCGGTGATTTGATCCTGACGGCGCGCAATCAGGAGCGTTTGGATAACCTGCAG
GCTGAACTCGGCCGGGGCAAGATTCTGCCCTTGGAAGCCGCTCTGCCGGAAGCTGACTTTATCGTG
TGGGTCGCCAGTATGCCTCAGGGCGTAGTGATCGACCCAGCAACCCTGAAGCAACCCTGCGTCCTA
ATCGACGGGGGCTACCCCAAAAACTTGGGCAGCAAAGTCCAAGGTGAGGGCATCTATGTCCTCAAT
GGCGGGGTAGTTGAACATTGCTTCGACATCGACTGGCAGATCATGTCCGCTGCAGAGATGGCGCGG
CCCGAGCGCCAGATGTTTGCCTGCTTTGCCGAGGCGATGCTCTTGGAATTTGAAGGCTGGCATACT
AACTTCTCCTGGGGCCGCAACCAAATCACGATCGAGAAGATGGAAGCGATCGGTGAGGCATCGGTG
CGCCACGGCTTCCAACCCTTGGCATTGGCAATTTGA

Table S3.2 Primers used in this chapter

Primers	Sequence
SeAR-SLiCE-F	5′-AAATTTAAGGAGCGATCGCCATGTTCGGT
	CTTATCGGTCATCTCACCAGTTTGGAGCAGG-3′
SeAR-SLiCE-R	5′-TCCATGTGCTGGCGTTCTCAAATTGCCAATG
	CCAAGGGTTGGAAGCCGTGGCGCACCGATGCC-3′
pRSF-Stag-F	5′-GAACGCCAGCACATGGACTCG-3′
pRSF-Stag-rbs-R	5′-GGCGATCGCTCCTTAAATTTCGCAGCAGCGGTTTCTTTACCAGA-3′
SeARseq-F	5′-GGCATCGACATTACCCAAGCGACAG-3′
SeARseq-R	5′-CTGTCGCTTGGGTAATGTCGATGCC-3′

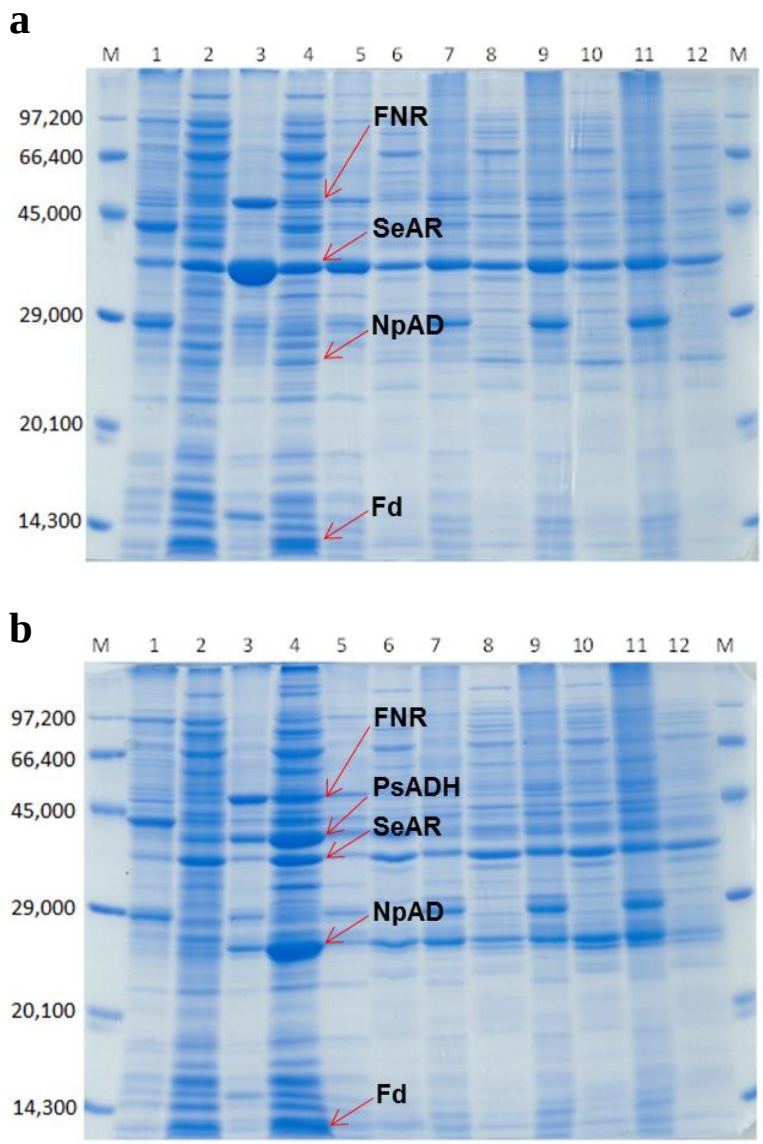

Figure S3.1 SDS-PAGE of the protein sampled from each time point during fermentative alkane production by (a) control strain and (b) ADH strain. The odd number lanes show the insoluble fractions, while the even number lanes show the soluble fraction. Lane 1–2: 3 h (before IPTG induction). Lane 3–4: 8 h. Lane 5–6: 24 h. Lane 7–8: 48 h. Lane 9–10: 72 h. Lane 11–12: 96 h. Lane M: standard molecular weight. The predicted sizes of target proteins are: 26,300 (NpAD), 37,500 (SeAR), and 39,500 (His-tagged PsADH).

CONCLUSION

In this study, the discovery of a fatty alcohol dehydrogenase, PsADH, was reported. This enzyme was found to be originated from a soil isolate of *Pantoea* sp. 7-4 strain during the screening of 1-tetradecanol-assimilating microorganisms. Heterologous expression of the *PsADH* gene in *E. coli* was conducted, and the recombinant PsADH was purified for a series of biochemical characterizations, including cofactors, optimal reaction conditions, kinetic parameters, and substrate specificity. PsADH was found to be NAD^+-dependent, with substrate specificity toward C6–C18 alcohols when catalyzing alcohol dehydrogenation reaction. Co-expression of PsADH with an aldehyde-deformylating oxygenase NpAD in *E. coli* resulted in the direct production of tridecane from 1-tetradecanol. By optimizing the reaction conditions for the constructed *E. coli* strain, the conversion rate of the reaction was increased to 52%. Furthermore, the alcohol-aldehyde-alkane synthetic route was applied to produce C5–C17 alkanes from their corresponding alcohol substrates. Finally, the effect of PsADH on fermentative alkane production was evaluated. This was achieved by co-expressing PsADH with NpAD and an acyl-ACP reductase SeAR and by cultivating the transformed *E. coli* strains in a jar fermenter. The introduction of PsADH led to the increase of alkanes and the decrease of fatty alcohol byproducts. The alkanes produced included tridecane, pentadecane, and heptadecene, which are expected to be used as drop-in biofuels.

ACKNOWLEDGEMENTS

This study is based on the work carried out from 2015 to 2017, and from 2019 to 2023 at the Laboratory of Fermentation Physiology and Applied Microbiology, Division of Applied Life Sciences, Graduate School of Agriculture, Kyoto University.

I would first like to appreciate Professor Jun Ogawa, who offers me the opportunities to study in this laboratory. His warm encouragement and invaluable advice support me throughout the course of this study and my life in Japan.

I would also like to express my sincere gratitude to Associate Professor Shigenobu Kishino, for his constant support and encouragement throughout the course of this study. His guidance helps me build up the ability to think scientifically and to solve problems when conducting research.

My gratitude also goes to Emeritus Professor Satomi Takahashi, Professor Makoto Ueda, Associate Professors Makoto Hibi and Ryotaro Hara, Assistant Professors Akinori Ando, Michiki Takeuchi and Hiroko Watanabe in Kyoto University, and Assistant Professor Yuta Sugiyama in Gunma University, for their kind advice and valuable instructions.

This study would not have been completed without Dr. Natsumi Okada, Dr. Si-Bum Park, Dr. Yoshimi Shimada, Dr. Tomoyo Okuda, Dr. Hideaki Nagano, Dr. Yoshie Fujiwara, Ms. Nahoko Kitamura, and Ms. Atsuko Kitamura. I would like to express my deep thanks for their kind instructions in experimental techniques, helpful advice, constant encouragement and unquestionable assistance.

I am grateful for the helpful suggestions and technical support provided by Dr. Masayoshi Muramatsu, Mr. Shusei Obata, and Mr. Masakazu Ito, Toyota Motor Corporation, throughout the course of this study.

Special thanks go to Mr. Satoshi Maruyama, for his great contribution to this study. Dr. Yuki Nakatani and Mr. Kousuke Fujii also contributed valuable information as previous work of this study. I would like to thank for their help.

I would like to thank Mr. Daichi Toyama, Mr. Takuma Morikawa, and Mr. Taiki Shiraishi, for bringing me helpful support and exciting experience throughout my life in Japan.

I appreciate Dr. Brian King Himm Mo, Dr. Daniel Makoto Takeuchi, Dr. Chang-Yu Wu, Mr. Makoto Sugimoto, and Mr. Kenta Nishitani, for discussing about my experiment results and sharing their life experience with me. Their suggestions make me become a better researcher and a better person.

I would also like to thank Dr. Sakuntala Saijai, Dr. Azusa Saika, Mr. Ryota Nakatsuji, Mr. Riku Usami, Mr. Wataru Shimada, Ms. Wakako Okada, Mr. Masafumi Horiki, Mr. Kensuke Ochi, Mr. Takayuki Iihoshi, Ms. Mariko Fujikawa, Ms. You-Shan Tsai, Mr. Yusaku Ehara, Ms. Thimira-Akari Yamamoto, Mr. Chun Wai Hui, Ms. Miu Kato, Mr. Ryota Kato, Mr. Shinya Nagahama, Mr. Kengo Deguchi, Mr. Taku Mizutani, Mr. Liang-Wei Wei, Mr. Chi Hei Ip, Ms. Juo-Ying Chen, Mr. Shota Kimoto, Mr. Naoki Ueda, Ms. Xinyang Liang, Ms. Julienne Hannelore Tolentino Borja, Ms. Anno Katasho, Ms. Rina Kawarada, Ms. Honoka Kitagawa, Ms. Moe Itoh, Mr. Taito Tsukimata, Mr. Hung-Cheng Lin, Mr. Yuichi Yoshimura, and all members of Laboratory of Fermentation Physiology and Applied Microbiology, Kyoto University.

Finally, I offer my deepest gratitude to my mom and dad, for their never-ending support, encouragement and understanding.

PUBLICATIONS

1. Yu-An Sui, Shigenobu Kishino, Satoshi Maruyama, Masakazu Ito, Masayoshi Muramatsu, Shusei Obata, Jun Ogawa. Utilizing alcohol for alkane biosynthesis by introducing a fatty alcohol dehydrogenase. *Appl. Environ. Microbiol.* **88**(23):e01264-22 (2022).

2. Yu-An Sui, Satoshi Maruyama, Natsumi Okada, Masakazu Ito, Masayoshi Muramatsu, Shusei Obata, Jun Ogawa, Shigenobu Kishino. Alkane production from fatty alcohols by the combined reactions catalyzed by an alcohol dehydrogenase and an aldehyde-deformylating oxygenase. In preparation.

3. Yu-An Sui, Satoshi Maruyama, Natsumi Okada, Masakazu Ito, Masayoshi Muramatsu, Shusei Obata, Shigenobu Kishino, Jun Ogawa. Application of a fatty alcohol dehydrogenase PsADH to fermentative production of alkanes. In preparation.